T cell activation induces proteasomal degradation of Argonaute and rapid remodeling of the microRNA repertoire

Yelena Bronevetsky,[1,2] Alejandro V. Villarino,[3] Christopher J. Eisley,[4] Rebecca Barbeau,[4] Andrea J. Barczak,[4] Gitta A. Heinz,[6] Elisabeth Kremmer,[6] Vigo Heissmeyer,[6] Michael T. McManus,[5] David J. Erle,[4] Anjana Rao,[7] and K. Mark Ansel[1,2]

[1]Sandler Asthma Basic Research Center, [2]Department of Microbiology and Immunology, [3]Department of Pathology, [4]Lung Biology Center, [5]University of California San Francisco Diabetes Center, University of California San Francisco, San Francisco, CA 94143
[6]Helmholtz Zentrum München, German Research Center for Environmental Health, Institute of Molecular Immunology, Munich, Germany 92037
[7]Division of Signaling and Gene Expression, La Jolla Institute for Allergy and Immunology, La Jolla, CA 50077

Activation induces extensive changes in the gene expression program of naive CD4+ T cells, promoting their differentiation into helper T cells that coordinate immune responses. MicroRNAs (miRNAs) play a critical role in this process, and miRNA expression also changes dramatically during T cell differentiation. Quantitative analyses revealed that T cell activation induces global posttranscriptional miRNA down-regulation in vitro and in vivo. Argonaute (Ago) proteins, the core effector proteins of the miRNA-induced silencing complex (miRISC), were also posttranscriptionally down-regulated during T cell activation. Ago2 was inducibly ubiquitinated in activated T cells and its down-regulation was inhibited by the proteasome inhibitor MG132. Therefore, activation-induced miRNA down-regulation likely occurs at the level of miRISC turnover. Measurements of miRNA-processing intermediates uncovered an additional layer of activation-induced, miRNA-specific transcriptional regulation. Thus, transcriptional and posttranscriptional mechanisms cooperate to rapidly reprogram the miRNA repertoire in differentiating T cells. Altering Ago2 expression in T cells revealed that Ago proteins are limiting factors that determine miRNA abundance. Naive T cells with reduced Ago2 and miRNA expression differentiated more readily into cytokine-producing helper T cells, suggesting that activation-induced miRNA down-regulation promotes acquisition of helper T cell effector functions by relaxing the repression of genes that direct T cell differentiation.

CORRESPONDENCE
K. Mark Ansel:
mark.ansel@ucsf.edu

Abbreviations used: Ago, Argonaute; dsRNA, double-stranded RNA; ES, embryonic stem; miRNA, microRNA; miRISC, miRNA-induced silencing complex; mTOR, mammalian target of rapamycin; PI3K, phosphatidylinositol 3-kinase; pri-miRNA, primary miRNA; pre-miRNA, precursor miRNA; qRT-PCR, quantitative real-time PCR; rRNA, ribosomal RNA; tRNA, transfer RNA.

During immune responses, antigen-specific CD4+ T cells undergo clonal expansion and differentiate into effector helper T cells that coordinate the immune response. Activation through TCR and co-stimulatory signals increases cellular metabolism to allow sufficient RNA and protein production to support cell growth, proliferation, and effector functions (Frauwirth and Thompson, 2004). Activated cells also become sensitive to signals that induce them to differentiate into distinct subsets of effector helper T cells, which perform specific immune functions through the selective production of cytokines (Zhu and Paul, 2010). For example, Th1 cells mediate immunity against intracellular infections by secreting IFN-γ, whereas Th2 cells use IL-4, IL-5, and IL-13 to orchestrate barrier immunity to control extracellular parasites (Szabo et al., 2003; Stetson et al., 2004). Lineage-restricted transcription factors, chromatin remodeling, and posttranscriptional regulation all contribute to the major changes in gene expression that characterize T cell activation and differentiation (Ansel et al., 2006; Wilson et al., 2009).

C.J. Eisley's present address is Dept. of Statistics, Iowa State University, Ames, IA.

The Rockefeller University Press $30.00
J. Exp. Med. 2013 Vol. 210 No. 2 417-432
www.jem.org/cgi/doi/10.1084/jem.20111717

The Journal of Experimental Medicine

MicroRNAs (miRNAs) are ∼22-nt single-stranded RNAs that direct posttranscriptional repression of many mRNAs, and thereby regulate diverse biological processes from cell proliferation and apoptosis to organ development and immunity (Hoefig and Heissmeyer, 2008; Bartel, 2009; Kim et al., 2009; O'Connell et al., 2010). miRNA genes are transcribed by RNA polymerase II, and the resulting primary miRNAs (pri-miRNAs) are processed by the Drosha–DGCR8 complex to produce ∼60–80-nt hairpin precursor miRNAs (pre-miRNAs). A second complex, consisting of Dicer and TRBP, cleaves pre-miRNAs to form small double-stranded RNA (dsRNA) duplexes, one strand of which becomes the mature miRNA upon loading into the miRNA-induced silencing complex (miRISC). Argonaute (Ago) proteins directly interact with miRNAs and are key factors in the assembly and function of the miRISC. miRNAs guide the miRISC to target mRNAs through direct base-pairing, leading to mRNA degradation and repression of protein expression.

T cells deficient in Dicer, Dgcr8, or Drosha, and thus lacking all miRNAs, exhibit decreased proliferation and survival and a propensity to rapidly differentiate into IFN-γ–producing effectors (Muljo et al., 2005; Cobb et al., 2006; Chong et al., 2008; Liston et al., 2008; Zhou et al., 2008; Steiner et al., 2011). Fully differentiated Th1 and Th2 cells express similar miRNA repertoires that are very distinct from that of naive T cells (Monticelli et al., 2005; Barski et al., 2009; Kuchen et al., 2010). Among the many miRNAs that change expression, there are several that regulate T cell clonal expansion or differentiation (Monticelli et al., 2005; Rodriguez et al., 2007; Thai et al., 2007; Xiao et al., 2008; Banerjee et al., 2010; Stittrich et al., 2010; Lu et al., 2010; Rossi et al., 2011; Steiner et al., 2011). Therefore, it is important to understand the mechanisms by which miRNA expression is regulated during T cell activation.

Some miRNA genes of importance in T cells are transcriptionally regulated by activation-induced transcription factors (Haasch et al., 2002; Taganov et al., 2006; Thai et al., 2007; Chang et al., 2008). However, discrepancies between pri-miRNA and mature miRNA abundance suggest that widespread posttranscriptional events also shape miRNA expression patterns in human lymphoma cell lines and mouse primary lymphocytes (Thomson et al., 2006; Kuchen et al., 2010). RNA-binding proteins can promote or repress processing of specific pri-miRNAs (Davis et al., 2008; Trabucchi et al., 2009). In addition, the stability and activity of the Drosha–DGCR8, Dicer–TRBP, and miRNA-induced silencing (miRISC) complexes are subject to regulation (Ghodgaonkar et al., 2009; Han et al., 2009; Paroo et al., 2009). Ago proteins in particular can undergo a variety of posttranslational modifications that affect their stability (Adams et al., 2009; Qi et al., 2008; Rybak et al., 2009; Rüdel et al., 2011). This is important because they can be a limiting factor for global miRNA expression levels (Diederichs and Haber, 2007; O'Carroll et al., 2007; Lund et al., 2011).

In this study, we show that miRNAs are globally down-regulated shortly after T cell activation. Through measuring miRNA precursors, we found that individual miRNAs are transcriptionally regulated upon T cell activation and that pri-miRNAs are efficiently processed into pre-miRNAs. We also measured miRNA biogenesis factors and determined that post-transcriptional down-regulation of Ago proteins occurs, mediated by ubiquitination and proteasomal degradation. This degradation depends on continuous signaling through the mammalian target of rapamycin (mTOR) pathway. Ago2 is a limiting factor in T cell miRNA homeostasis, and Ago2-deficient T cells exhibit increased differentiation into cytokine-producing effectors. Thus, miRNA expression in activated T cells is globally regulated at the posttranscriptional level, likely through increased miRISC turnover. This, together with miRNA gene-specific transcriptional changes, rapidly resets the miRNA repertoire during T cell activation.

RESULTS

T cell activation induces widespread miRNA down-regulation

We previously showed that helper T cell differentiation is associated with major changes in miRNA expression (Monticelli et al., 2005). To determine the kinetics with which these changes occur, we measured miRNA expression during a time course of T cell activation. Spleen and lymph node $CD4^+$ cells were stimulated with plate-bound anti-CD3 and -CD28 for 3 d, and then rested in media containing IL-2 until day 7. Equal quantities of RNA from cells harvested at various time points were subjected to Northern blot analysis. As expected, T cell activation induced an increase in the total RNA yield per cell, and the relative expression of ribosomal RNA (rRNA) remained stable throughout the time course (Fig. 1 A). Although many "housekeeping" mRNA transcripts, including miRNA targets, are induced upon T cell activation, rRNA makes up a constant proportion of cellular RNA across many cell types and experimental conditions (Bas et al., 2004). The 5.8S, 18S, and 28S rRNAs are co-transcribed and processed from a single precursor and maintained at a constant stoichiometric ratio with each other and the 5S rRNA. Transfer RNA (tRNA) abundance also tracked closely with 5.8S rRNA in activated T cells (Fig. 1 A). Therefore, we used rRNAs as a standard for normalization throughout this study, with attention to matching the size of the standard and analytes in each assay. Consistent with previous studies, miR-155 was up-regulated in activated T cells, whereas miR-150 and miR-146 were down-regulated (Monticelli et al., 2005; Rodriguez et al., 2007; Thai et al., 2007; Banerjee et al., 2010). Surprisingly, several other miRNAs were also down-regulated (Fig. 1 A and not depicted), including miRNAs that are highly expressed throughout the T cell lineage (e.g., miR-142), and several miRNAs that are expressed broadly in mouse tissues (e.g., miR-16). miRNA expression decreased within 4 h of activation, and the largest reduction was observed by 44 h (Fig. 1 A and not depicted).

We measured the expression of all miRNAs across a time course of T cell activation using miRNA microarrays. Microarray data are typically normalized using quantile normalization

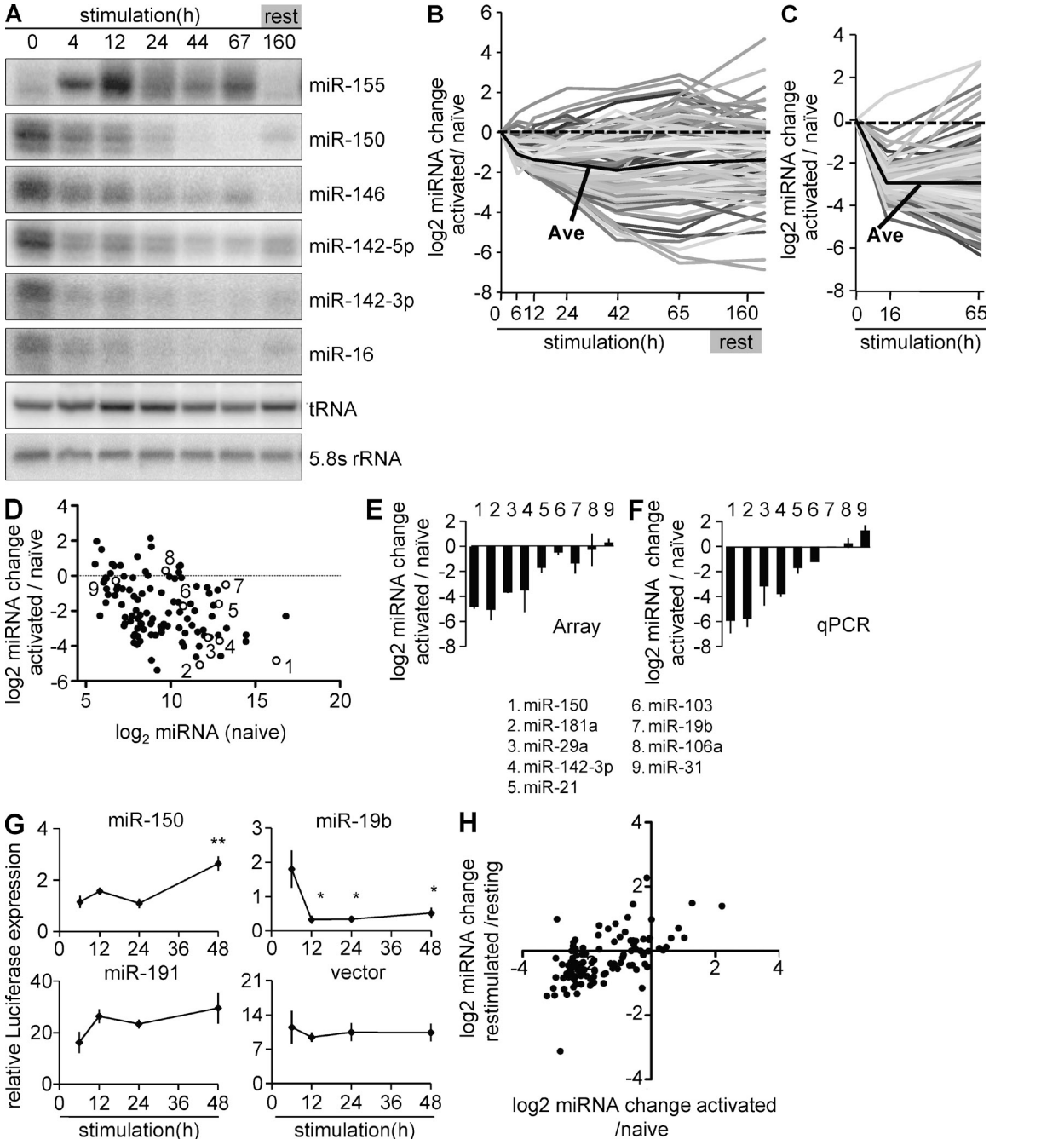

Figure 1. T cell activation leads to global miRNA depletion. (A) Northern blot analysis of indicated miRNAs in naive CD4+ T cells, and CD4+ T cells stimulated for the indicated amounts of time with anti-CD3 and anti-CD28. tRNA and 5.8S rRNA are used as loading controls. (B) Array analysis of 114 miRNAs in naive CD4+ T cells, and CD4+ T cells stimulated for the indicated amounts of time with anti-CD3 and anti-CD28. Data are relative to naive cells and were normalized to tRNA. (C) Array analysis of 174 miRNAs in naive human peripheral blood CD4+ T cells and CD4+ T cells stimulated with anti-CD3 and anti-CD28. Data are relative to naive, normalized to tRNA. (D) miRNA expression in naive and 48 h in vitro–activated T cells. The x axis denotes raw intensity of all probes in the naive group and y axis denotes the fold difference between activated and naive groups, normalized to tRNA (Log2) Open circles with numbers correspond to chart in E and F. (E) Bar graph denotes expression of selected miRNAs in the activated group as measured by array normalized to tRNA. (F) Bar graph denotes expression of selected miRNAs in the activated group as measured by qRT-PCR normalized to 5.8S rRNA. (G) Relative Luciferase activity from sensors for miR-150, 19b, 191, and vector control at indicated times. Data are the mean of at least five replicates and four independent experiments. *, $P < 0.05$; **, $P < 0.01$, two-way ANOVA. (H) Log2 fold difference between 24-h activated and naive T cells (x-axis) and log2 fold difference between 24-h restimulated and resting T cells (Y-axis). Data are representative of at least two independent experiments.

or other algorithms that adjust the hybridization intensity of each probe relative to the intensity of all other probes on the array. This approach yields information about the expression of each miRNA relative to the other miRNAs in a sample, but it fails to capture global changes in the expression of miRNAs as a class. Therefore, we customized our arrays to include probes for several control noncoding RNAs, including tRNAs. Compared with tRNA, global miRNA expression decreased measurably within 12 h of T cell activation, long before any cell division has occurred. Within 2 d, a large majority of all expressed miRNAs were down-regulated, with a mean reduction to less than 25% of that seen in naive T cells (Fig. 1 B). Very similar results were obtained using naive $CD4^+$ T cells isolated from human peripheral blood (Fig. 1 C).

We confirmed the array data by quantitative real-time PCR (qRT-PCR) measurement of a panel of miRNAs with a range of expression in T cells (Fig. 1, D–F). As shown in the array, the abundance of most miRNAs decreased relative to tRNA in T cells activated for 42 h (Fig. 1 E). Because qRT-PCR does not suffer from the data compression inherent in hybridization-based array analyses, it provides a more accurate measure of the magnitude of miRNA down-regulation (Shi et al., 2006). The most highly down-regulated miRNAs, miR-150, and miR-181a, decreased to less than 2% of their abundance in naive T cells (Fig. 1 F).

To directly monitor miRNA activity during T cell activation, we constructed slicer-dependent miRNA sensors with perfectly complementary miRNA-binding sites cloned downstream of *Renilla* luciferase (Fig. 1 G). T cells were transfected with sensors for miR-150 (most highly down-regulated), miR-191 (moderately down-regulated), miR-19b (up-regulated), or a control vector without miRNA-binding sites. Primary T cells were transfected at various times after stimulation, and luciferase activity was measured 18 h later. These experiments revealed the expected reciprocal relationship between sensor activity and miRNA expression. As miR-150 and miR-191 levels decreased, their luciferase sensors exhibited increased luciferase activity. Conversely, as miR-19b expression increased, there was a decrease in luciferase activity from this sensor. The vector control exhibited no significant change in luciferase activity over the time course of activation.

Finally, we asked if resting T cells would exhibit similar miRNA down-regulation upon restimulation. T cells were rested until day 6, and then restimulated on plate-bound anti-CD3 and -CD28 for 24 h. Microarray profiling revealed that restimulated cells display a pattern of miRNA expression changes similar to that seen in naive T cells stimulated for the first time (Fig. 1 H). Thus, restimulation of resting in vitro–derived effector T cells recapitulates the activation-induced down-regulation of most miRNAs.

Activation-induced down-regulation of Ago proteins

To explore the possibility that activation-induced miRNA down-regulation could be the result of reduced expression of key proteins in the miRNA biogenesis pathway, we measured Drosha, Dicer, and TRBP during T cell activation. The mRNA of the genes encoding all three proteins were induced to varying degrees within 14 h, and then returned to baseline in resting T cells (Fig. 2 A). The abundance of Drosha and Dicer protein followed the same pattern with a slight delay. Both exhibited strong induction followed by a return to baseline levels (Fig. 2 B). In contrast, increased TRBP protein expression persisted even when T cells were removed from stimulus and allowed to rest in IL-2–containing media for >3 d. The induction of these miRNA biogenesis proteins in activated T cells is interesting, but it cannot account for the concurrent reduction in mature miRNA expression.

Ago protein abundance has emerged as a common limiting factor that determines miRNA levels, and Ago stability and miRNA-binding activity are subject to regulation by posttranslational modification (Diederichs and Haber, 2007; O'Carroll et al., 2007; Qi et al., 2008; Adams et al., 2009; Rybak et al., 2009; Lund et al., 2011). Like Drosha, Dicer, and TRBP, Ago1, Ago2, and Ago3 were moderately induced at the transcriptional level by 14 h (Fig. 2 C). Ago4 mRNA could not be detected in these cells. Ago1 and Ago2 protein expression did not follow the same pattern, instead resembling the kinetics of miRNA down-regulation in activated T cells. Ago1 and Ago2 decreased significantly within 24 h, reached a minimum at 48 to 72 h of activation, and remained very low for the remainder of the time course (Fig. 2 D). Probing with a new monoclonal antibody that recognizes all four mouse Ago proteins (Fig. S1 A) revealed a similar pattern for total Ago protein expression (Fig. 2 E).

To determine whether Ago protein abundance is a limiting factor for global miRNA homeostasis in T cells, we measured miRNA levels in Ago2-deficient T cells. Spleen and lymph nodes of *Ago2$^{fl/fl}$; CD4-cre* mice and their *Ago2$^{+/+}$; CD4-cre* (WT) littermates contained similar numbers of $CD4^+$ and $CD8^+$ T cells, and similar proportions of naive ($CD62L^{hi}CD44^{lo}$) and memory ($CD62L^{lo}CD44^{hi}$) cells (Fig. 3 A). Western blot analysis confirmed the absence of Ago2 protein in bead-sorted T cells from *Ago2$^{fl/fl}$; CD4-cre* mice (Fig. 3 B). Importantly, miRNA expression was also significantly lower in these cells (Fig. 3 C). 23 out of 24 members of a panel of T cell–expressed miRNAs were decreased by an average of 60% in *Ago2$^{fl/fl}$; CD4-cre* T cells, and 30% in heterozygous *Ago2$^{+/fl}$; CD4-cre* T cells relative to 5.8S rRNA. Other noncoding small RNAs, small nucleolar RNA-202 and U7 small nuclear RNA, were unaffected. The remaining miRNAs may be associated with other Ago family proteins. To further test if Ago proteins are limiting for T cell miRNA expression, we re-expressed Ago2 in differentiating Ago2-deficient T cells. Cells were transduced with Ago2 or control retrovirus at 80–90% efficiency as measured by expression of the GFP marker gene (unpublished data). Ago2 protein was detected only in Ago2-transduced cells (Fig. 3 D). miRNA expression increased in these cells by an average of 145% (Fig. 3 E). These results demonstrate that miRNA expression in T cells is highly sensitive to changes in Ago protein expression, and indicate that activation-induced

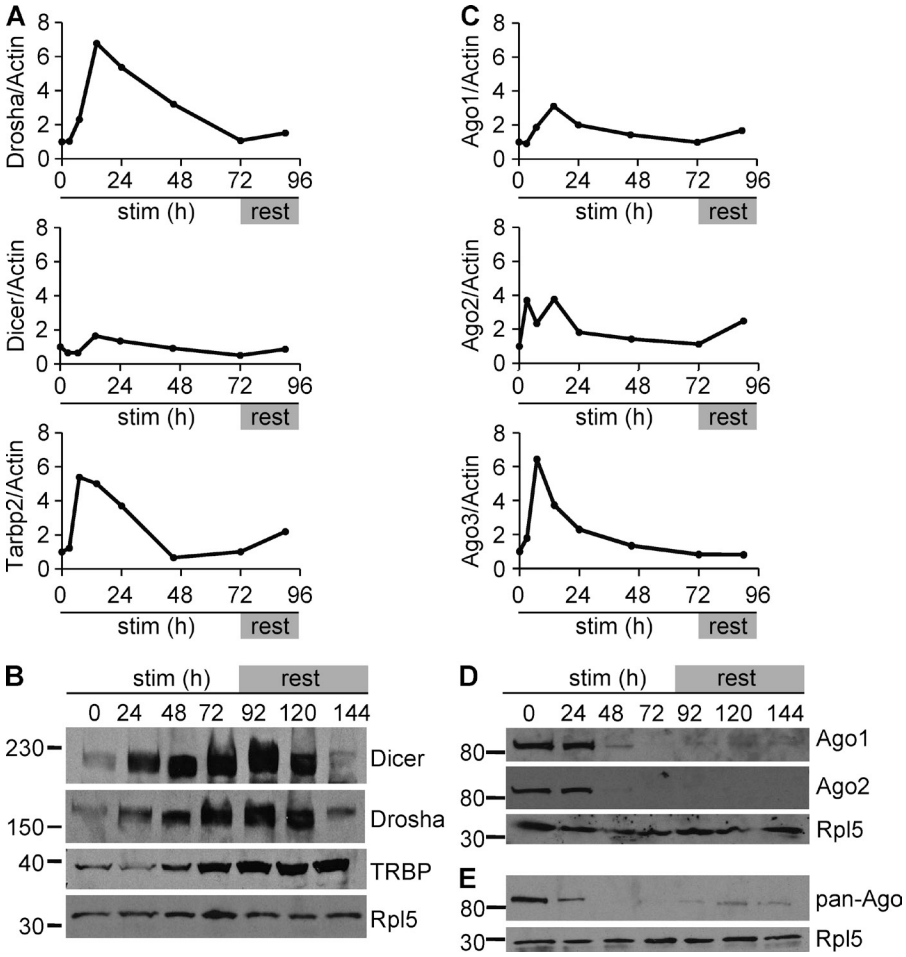

Figure 2. Ago proteins are posttranscriptionally down-regulated upon T cell activation. (A) qRT-PCR analysis of indicated mRNAs in naive and stimulated CD4+ T cells. Data are normalized to β-actin. (B) Immunoblot analysis of indicated proteins in naive and stimulated CD4+ T cells. Rpl5 serves as a loading control. (C) qRT-PCR analysis of Ago1, Ago2, and Ago3 in naive and stimulated CD4+ T cells. Data are normalized to β-actin. (D) Immunoblot analysis of Ago1 and Ago2 in naive and stimulated CD4+ T cells. Rpl5 serves as a loading control. (E) Immunoblot analysis of pan-Ago in naive and stimulated CD4+ T cells as in D. PCR data are the mean of two duplicate reactions. Data are representative of at least three experiments.

down-regulation of Ago1 and Ago2 could be the proximate cause of the observed decrease in mature miRNA expression in activated T cells.

miRNAs restrain helper T cell differentiation and cytokine production

Dicer-, *Drosha*-, or *Dgcr8*-deficient T cells that lack all miRNAs undergo abnormally rapid and robust differentiation into cytokine-producing effector cells upon activation (Muljo et al., 2005; Chong et al., 2008; Liston et al., 2008; Steiner et al., 2011). However, these cells also expand poorly because of reduced proliferation and increased apoptosis. In contrast, activated Ago2-deficient and heterozygous T cells divided at a similar rate as control cells, and expanded to similar cell numbers in in vitro cultures (Fig. 4 A and not depicted). This indicates that T cell proliferation does not require the "slicer" activity of Ago2 that mediates RNA interference, and allowed us to test for proliferation and survival-independent effects of reduced miRNA expression on T cell differentiation and cytokine production. CD4+ T cells were activated for 3 d in conditions that drive Th1 (10 ng/ml IL-12, anti–IL-4) or Th2 (500 U/ml IL-4, anti–IFN-γ) differentiation, in limiting concentrations of IL-4 (10 U/ml) or IL-12 (10 pg/ml), and in nonpolarizing conditions (ThN; no cytokines or blocking antibodies added). They were allowed to rest for 3 d in the presence of IL-2, and then restimulated to induce cytokine production. The percentage of cytokine-producing cells increased in all conditions tested (Fig. 4 B). In nonpolarizing conditions, a 70% increase in the proportion of IFN-γ–producing cells was coupled with a significant increase in the Th2 cytokines IL-4 and IL-13. Very similar results were obtained with limiting IL-12, and Th2 cytokines were increased even in strong Th1- and Th2-polarizing conditions. In limiting IL-4 conditions, there was a significant increase in the production of all three cytokines. Thus, Ago2-deficient T cells produced more lineage-specific effector cytokines without a particular bias toward Th1 or Th2 differentiation. These data indicate that miRNAs are required in naive T cells to restrain their differentiation. When miRNAs are depleted, as in the case of Ago2 deficiency, cells are more likely to differentiate into cytokine-producing effectors.

The pathways and specific mRNAs targeted by miRNAs to restrain T cell differentiation and cytokine production are mostly unknown and likely complex. However, as an example of a relevant established miRNA target, we also measured the expression of T-bet in differentiating Ago2-deficient T cells

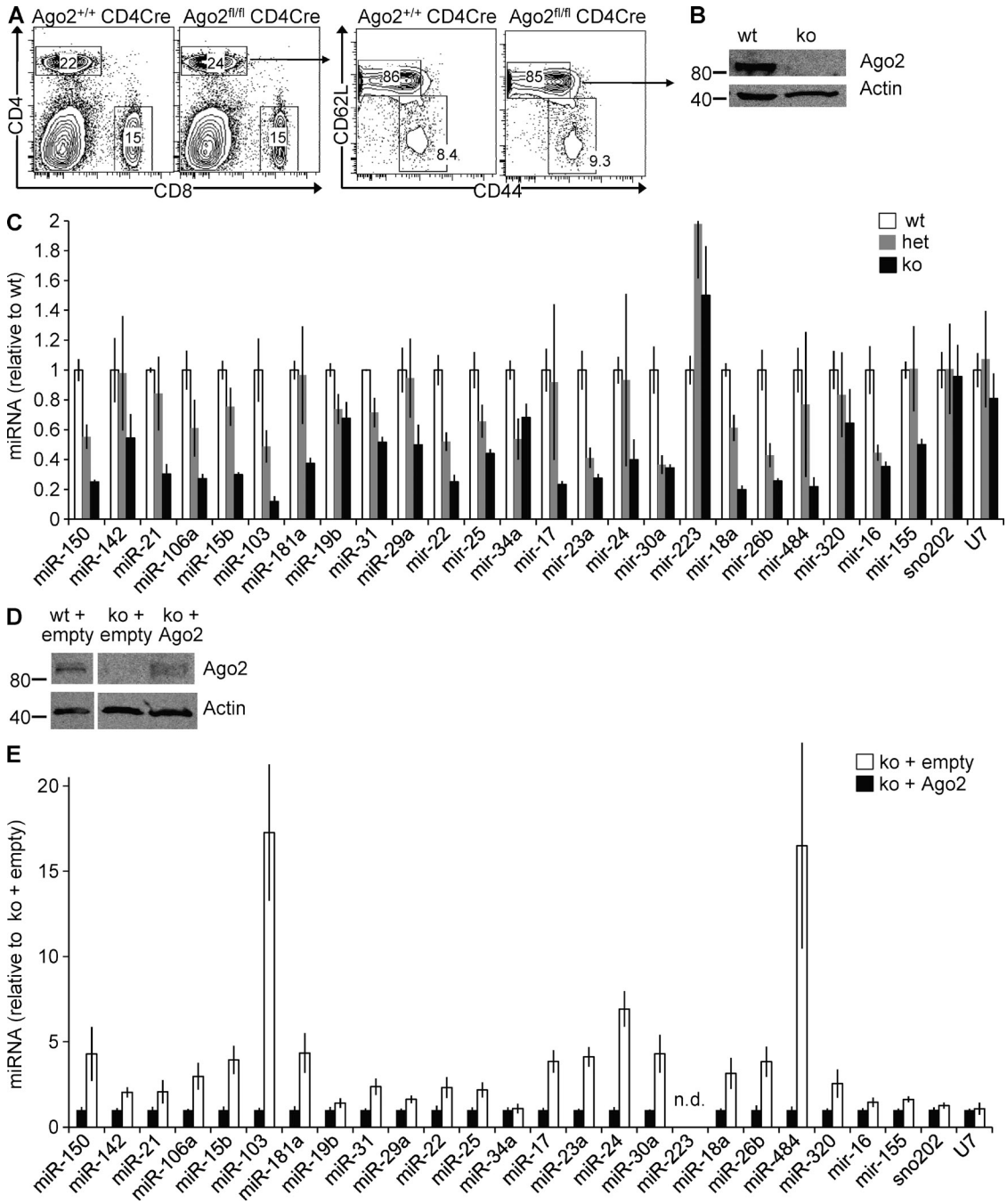

Figure 3. Ago2 is limiting for T cell miRNA expression. (A) Flow cytometry analysis of staining for CD4 and CD8 (left) in mixed spleen and lymph nodes from 4–6-wk-old *Ago2*$^{+/+}$; *CD4-cre* and *Ago2*$^{fl/fl}$; *CD4-cre* mice. Flow cytometry analysis of staining for CD62L and CD44 (right) in mixed spleen and lymph nodes. (B) Immunoblot analysis of Ago2 in naive CD4$^+$ T cells from *Ago2*$^{+/+}$, and *Ago2*$^{fl/fl}$; *CD4-cre* mice. β-Actin serves as a loading control. (C) qRT-PCR analysis of indicated miRNAs in naive CD4$^+$ T cells from *Ago2*$^{+/+}$, *Ago2*$^{+/fl}$ and *Ago2*$^{fl/fl}$; *CD4-cre* mice. Data are normalized to 5.8S, and are represented relative to WT. (D) Immunoblot analysis of Ago2 in 6-d cultured *Ago2*$^{+/+}$ and *Ago2*$^{fl/fl}$; *CD4-cre* CD4$^+$ T cells transduced on day 2 with Ago2 retrovirus or empty retrovirus control. (E) qRT-PCR analysis of indicated miRNAs in 6-d cultured *Ago2*$^{fl/fl}$; *CD4-cre* CD4$^+$ T cells transduced on day 2 with Ago2 retrovirus or empty retrovirus control. Data are representative of three experiments, and error bars represent standard error of the mean. n.d., not detected.

(Fig. 4 C). T-bet is a key transcription factor required for Th1 differentiation recently shown to be a direct target of miR-29 in T cells (Steiner et al., 2011) T-bet expression increased in Ago2-deficient cells in nonpolarizing, limiting IL-4 and limiting IL-12 conditions. No differences were evident in Th1 conditions, which presumably have maximal T-bet expression,

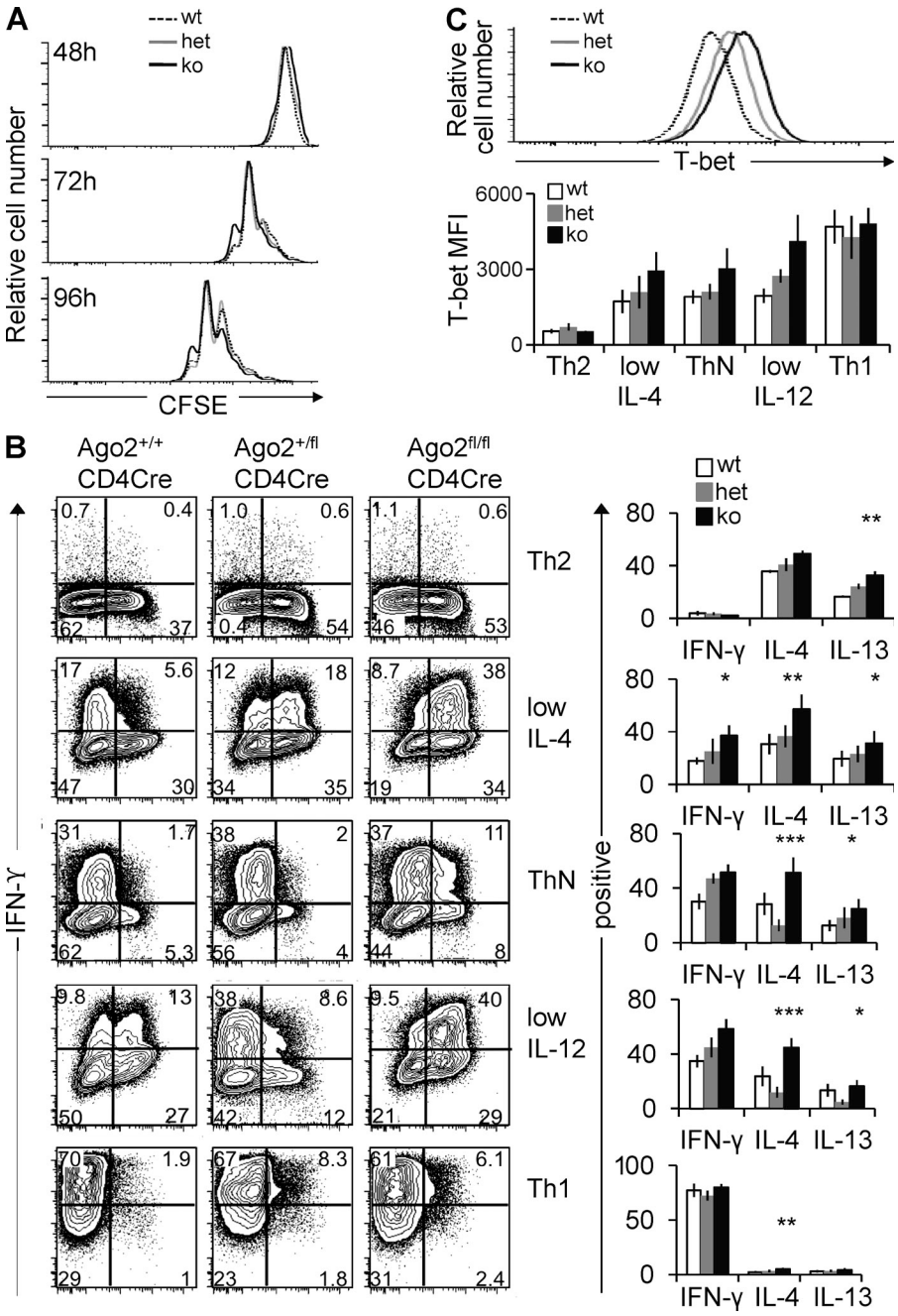

Figure 4. Increased effector cytokine production in Ago2-deficient T cells. (A) Flow cytometry analysis of staining for CFSE in CD4+ T cells cultured for the indicated times in nonpolarizing conditions. (B) Flow cytometry analysis (left) of intracellular staining for IFN-γ and IL-4 production by restimulated T cells isolated from *CD4-cre Ago2*$^{fl/fl}$ (ko), *Ago2*$^{+/fl}$ (het) or *Ago2*$^{+/+}$ (wt) mice differentiated for 1 wk under Th2, low IL-4, ThN, low IL-12, and Th1 conditions. Numbers indicate percentage of cells in each quadrant. Bar graphs (right) show percentage of CD4+ cells producing IFN-γ, IL-4, and IL-13 in the conditions on the left. *, $P < 0.05$; **, $P < 0.01$; ***, $P < 0.001$, two-way ANOVA. (C) Flow cytometry analysis (top) of intracellular staining for T-bet in T cells differentiated for 1 wk in low IL-12 conditions. Bar graphs (bottom) show T-bet mean fluorescence intensity (MFI) in CD4+ cells under Th2, low IL-4, ThN, low IL-12, and Th1 conditions. Data are representative of three experiments, and error bars represent standard error of the mean.

or in Th2 conditions in which both T-bet and IFN-γ expression is very low. Thus, the increased T-bet in Ago2-deficient cells correlates with increased IFN-γ in those cells (Fig. 4, B and C), and may directly contribute to this effect.

Specific transcriptional changes and global posttranscriptional down-regulation reset the miRNA repertoire in activated T cells

Down-regulation of Ago proteins could plausibly account for the widespread reduction in miRNA abundance in activated T cells. This mechanism would be unlikely to act in a miRNA-specific fashion. However, we observed significant heterogeneity in the expression of individual miRNAs in response to T cell activation, indicating that one or more additional layers of regulation remodel the miRNA repertoire during T cell differentiation (Fig. 1 B). Specifically, we identified three groups of miRNAs for further investigation: (1) miRNAs such as miR-150, which are heavily down-regulated, decreasing to 1–2% of their starting levels during T cell activation (Fig. 5 A, top); (2) miRNAs like miR-106a that remain at relatively constant abundance or are slightly up-regulated (Fig. 5 A, middle); and (3) the largest group of miRNAs that are moderately down-regulated to the global mean of ∼25% of their starting abundance (Fig. 5 A, bottom).

To determine whether miRNA gene-specific transcriptional regulation may explain these different expression patterns, we measured the corresponding pri-miRNAs. pri-miRNAs whose corresponding mature miRNA exhibited the greatest down-regulation also fell precipitously during T cell activation, reaching 3–10% of their starting levels within 24 h (Fig. 5 B, top). These data suggest that miRNAs in this class are regulated by activation-induced repression of pri-miRNA transcription. However, a posttranscriptional mechanism also appears to contribute, as the mature miRNAs were down-regulated further and faster than can be accounted for by transcriptional repression alone. miRNAs with levels that increased or remained unchanged during T cell activation exhibited robust up-regulation of at least one of their corresponding pri-miRNAs (Fig. 5 B, middle). For these miRNAs, the magnitude of pri-miRNA induction exceeded miRNA up-regulation by 4–20-fold, suggesting that these miRNAs are also subject to posttranscriptional down-regulation even as they are transcriptionally induced. In addition, pri-miRNAs corresponding to miRNAs that were moderately down-regulated during activation did not exhibit decreased expression, but instead exhibited an early transient increase, followed by a return to baseline levels for the remainder of the time course (Fig. 5 B, bottom). Collectively, these findings indicate that miRNA-specific transcriptional regulation is layered over a global posttranscriptional mechanism of down-regulation. Together, these mechanisms allow rapid changes in the miRNA expression patterns of activated T cells that are entering a phase of growth and differentiation.

In addition to changes in miRISC stability and regulation of miRNA gene transcription, we investigated the possibility that activated T cells may exhibit a block in the enzymatic steps in miRNA biogenesis. To this end, we assayed pre-miRNA abundance during an activation time-course. Because pre-miRNAs share their entire sequence with the corresponding pri-miRNA, we devised a method to distinguish them in qRT-PCR assays by separating cellular RNA into small (<200 nt) and large (>200 nt) fractions. Two primers that bind to the stem loop sequence were then used to measure pre-miRNAs in the small RNA fraction (Fig. 6 A, right). pri-miRNAs can be unambiguously detected using PCR primers spanning the Drosha cleavage site in the miRNA-containing stem–loop structure (Fig. 6 A, left). pri-miRNA–specific primers amplified their product from the large fraction, but

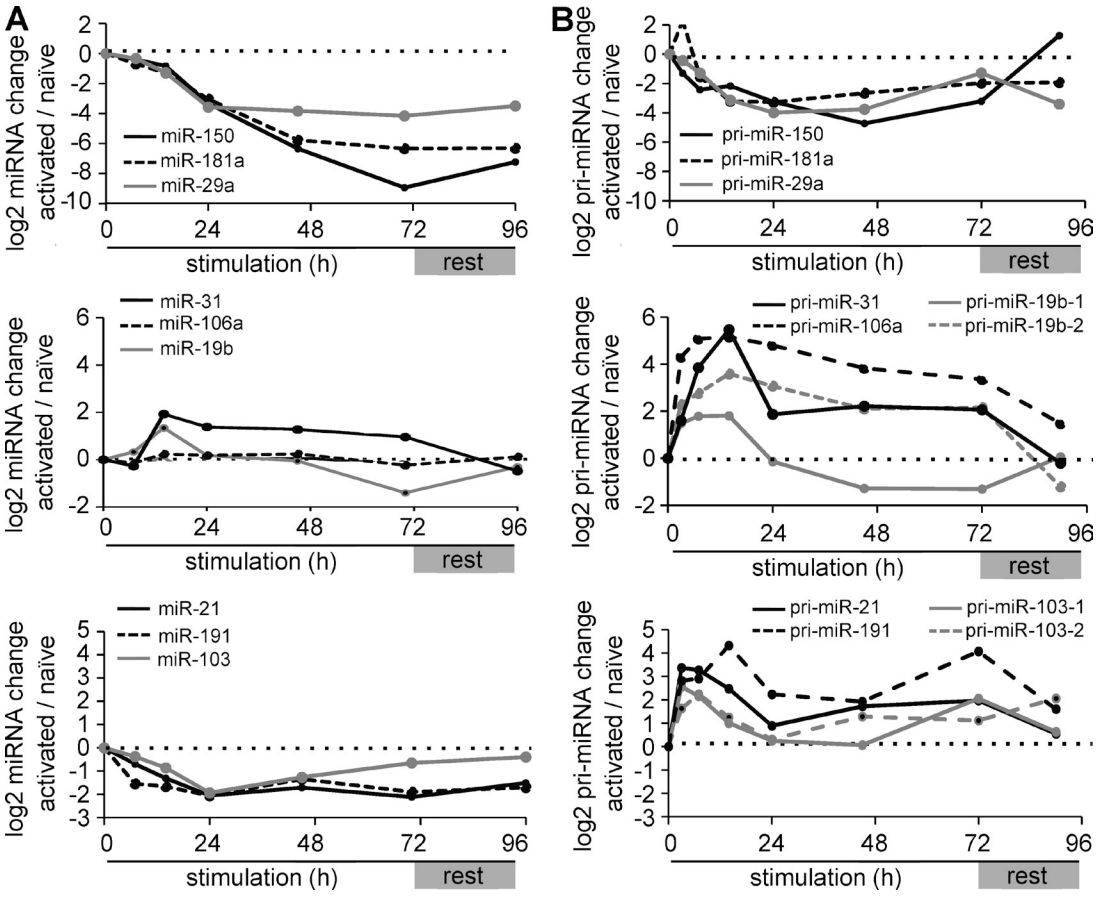

Figure 5. Activation-induced transcriptional regulation leads to differential expression of mature miRNAs. (A) Quantitative PCR analysis of indicated miRNAs in naive and stimulated CD4+ T cells. Data are relative to naive, normalized to 5.8S rRNA. (B) PCR analysis of indicated pri-miRNAs in naive and stimulated CD4+ T cells. Data are normalized to 28S rRNA. qRT-PCR data are representative of 10 experiments.

no product was detected in the small RNA fraction, indicating that pri-miRNAs were effectively removed (Fig. 6 B, left). pre-miRNA primers amplified a product in both fractions (Fig. 6 B, right). Both pri-miRNA and contaminating pre-miRNAs may contribute to the products amplified from the large fraction, but pre-miRNA abundance could be specifically measured in the small fraction. We routinely confirmed the absence of the corresponding pri-miRNAs in the small fraction when measuring pre-miRNAs.

If pri-miRNA processing to pre-miRNA were blocked in activated T cells, pre-miRNA expression would be expected to fall rapidly during an activation time course. If pre-miRNA to miRNA expression were blocked, some pre-miRNAs would be expected to accumulate, as has been shown for pre-miR-21 and pre-miR-150 in Dicer-deficient CD4$^+$ T cells (Muljo et al., 2005). However, pre-miR-21 expression consistently tracked closely behind pri-miR-21 expression across the activation time-course. Pri-miR-21 was transiently up-regulated during the first 6 h of activation, and a corresponding transient increase in pre-miR-21 was observed at 12 h (Fig. 6 C). In contrast, mature miR-21 was clearly down-regulated within 24 h of T cell activation. Even during the early burst of pri-miR-21 transcription and processing, mature miR-21 remained at or below its concentration in naive T cell. We confirmed these data by Northern blot using a miR-21–specific probe that recognizes both mature and pre-miR-21 (Fig. 6 D). Pre-miR-150 was detected only in naive T cells, which is consistent with transcriptional silencing (unpublished data). We conclude that neither Drosha nor Dicer processing is blocked in activated T cells, though the processing efficiency of specific miRNAs could be subject to regulation.

In vivo–activated T cells exhibit global miRNA down-regulation

We also investigated whether similar miRNA regulation occurs in T cells activated in vivo. OVA-specific, TCR-transgenic naive CD4$^+$ T cells were adoptively transferred into WT congenic hosts, some of which were then immunized with OVA-pulsed DCs. At 5 d after transfer, CD44^{hi} effector CD4$^+$ T cells were purified from immunized mice, and naive cells were recovered from unimmunized mice (Fig. S2). Quantitative PCR showed that miRNAs were also down-regulated in T cells activated in vivo (Fig. 7 A and not depicted). Microarray analysis showed close correlation between the miRNA expression changes induced in effector T cells in vivo and those induced by activation in vitro for 65 h (Fig. 7 B). In vivo–activated T cells also down-regulated Ago2 protein to an extent similar to that observed in vitro, with the protein becoming almost undetectable (Fig. 7 C). Collectively, these data demonstrate that Ago protein and global miRNA down-regulation occur in physiologically relevant T cell responses.

Ago2 is ubiquitinated and degraded by the proteasome

Finally, we investigated the mechanism of activation-induced Ago2 down-regulation. To make biochemical analyses more

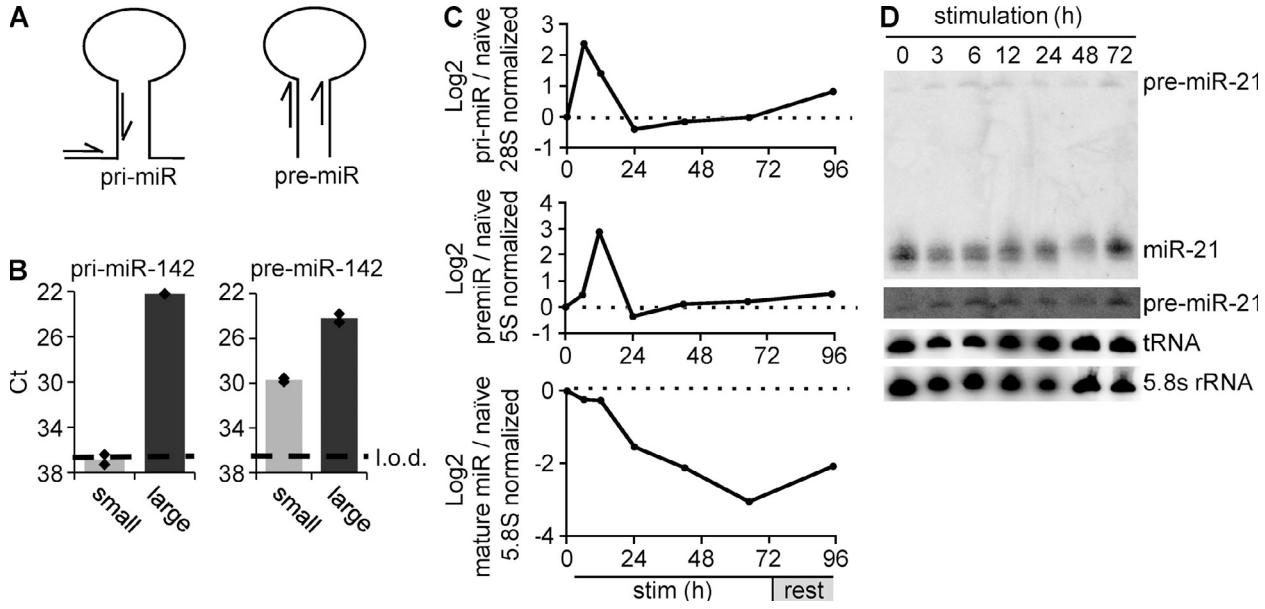

Figure 6. Efficient miRNA processing occurs in activated T cells. (A) Graphical representation of pri-miRNA and pre-miRNA primers shows those spanning one arm of the stem loop and the flanking sequence (pri-miR), and those within the stem loop (pre-miR). (B) Validation of size fractionation technique shows thermal cycle (Ct) values for qRT-PCR performed with pri-miR-142 and pre-miR-142 primers in the small and large RNA fractions. Dotted line represents limit of detection. (C) qRT-PCR analysis of pri-, pre-, and mature miR-21 in naive and stimulated CD4$^+$ T cells. Data are relative to naive, normalized to 28S rRNA (pri-miRNA), 5S rRNA (pre-miRNA), and 5.8S rRNA (mature miRNA). Data in A–C are representative of five experiments. (D) A Northern blot analysis of pre- and mature miR-21, tRNA, and 5.8S rRNA in naive CD4$^+$ T cells and CD4$^+$ T cells stimulated for the indicated amounts of time with anti-CD3 and anti-CD28. Bottom pre-miR-21 panel is a higher exposure.

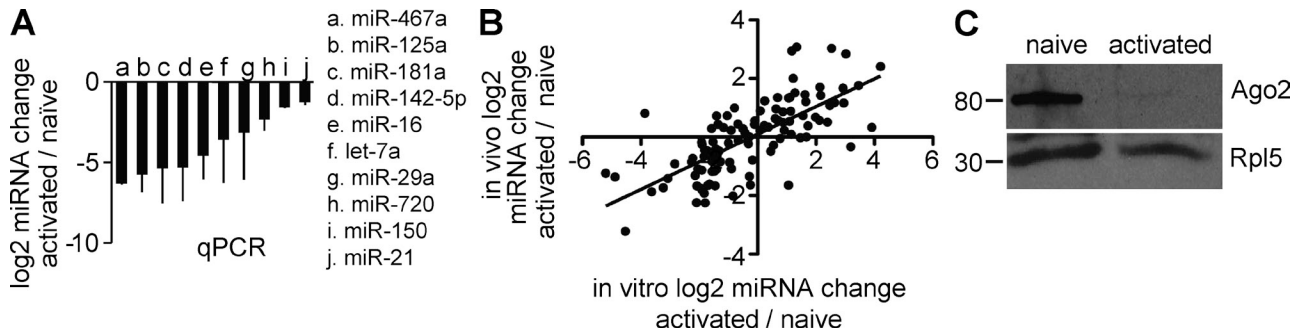

Figure 7. miRNA depletion and Ago2 down-regulation occurs during in vivo T cell activation. (A) miRNA expression in in vivo activated OVA-specific T cells as measured by qRT-PCR normalized to 18S rRNA. Data are representative of at least five experiments, and error bars indicate the standard deviation between replicate measurements. (B) Log2 fold difference between in vivo activated and naive T cells (y axis) and log2 fold difference between 65h in vitro–activated and naive T cells (x axis). (C) Immunoblot analysis of Ago2 and RPL5 protein in naive and in vivo–activated, OVA-specific T cells. Data are representative of two independent experiments.

feasible, we performed our studies in in vitro–cultured T cells, which down-regulated miRNAs upon restimulation with anti-CD3 and -CD28 (Fig. 1 H). Ago2 was also down-regulated in restimulated cells, reaching nearly undetectable levels within 24 h (Fig. 8 A). As previous studies have indicated that Ago2 can be ubiquitinated and degraded by the proteasome, we wondered whether this mechanism occurs in activated T cells (Adams et al., 2009; Rybak et al., 2009). Treatment with MG-132 during the final 2 h of restimulation largely restored Ago2 protein abundance to the quantity found in unstimulated cells. This finding shows a critical role for the proteasome in Ago2 down-regulation, and indicates that Ago2 undergoes a high rate of turnover in activated T cells.

Next, we tested whether Ago2 itself becomes ubiquitinated during T cell activation. T cells were restimulated or left at rest in media supplemented with MG-132 for the final 4 h to stabilize ubiquitinated proteins, and lysates were prepared under stringent conditions that disrupt noncovalent protein interactions. Anti-Ago2 immunoprecipitates from activated T cells contained an accumulation of high molecular mass forms of immunoprecipitated Ago2 (>90 kD) that were recognized by ubiquitin immunoblotting (Fig. 8 B). Ubiquitinated Ago2 was far less abundant in resting T cells, and was not detected in control immunoprecipitations with nonspecific antibody. Importantly, the high molecular mass proteins that we identified as ubiquitinated Ago2 were detected in restimulated WT T cells, but not in Ago2-deficient T cells (Fig. 8 C). To confirm these results with an independent antibody for immunoprecipitation, we transduced WT T cells with HA-tagged Ago2. Like the endogenous protein, retrovirally encoded HA-Ago2 was down-regulated upon T cell activation in an MG132-sensitive manner (Fig. 8 D). In addition, anti-HA specifically immunoprecipitated ubiquitinated proteins with high molecular masses only in restimulated cells expressing HA-Ago2 (Fig. 8 E). Ago2 ubiquitination could be detected as early as 12 h after stimulation (Fig. 8 F). These data strongly support a model in which T cell activation induces ubiquitination and proteasomal degradation of Ago2, and probably other Ago proteins as well.

We asked which signals downstream of TCR engagement are required for Ago2 down-regulation. Inhibition of proximal TCR signaling with the Src-family kinase inhibitor PP2 partially rescued Ago2 protein expression (Fig. 9 A). A robust increase in Ago2 was observed in cells activated in the presence of the phosphatidylinositol 3-kinase (PI3K) inhibitor LY294002 (Fig. 9 A) or the mTOR inhibitor rapamycin (Fig. 9 B). LY294002 is also a potent inhibitor of mTOR (Brunn et al., 1996). In contrast, calcineurin and MAPK activity were dispensable, as blocking these pathways with Cyclosporin A or U0126, respectively, had no effect on Ago2 down-regulation (Fig. 9 B). Continuous mTOR signaling was required to maintain low Ago2 expression because rapamycin treatment restored it to unstimulated T cell levels within 2 h (Fig. 9 C).

Treatment with actinomycin D or cycloheximide also rapidly rescued Ago2 expression (Fig. 9 D), indicating that continued transcription and translation are required for Ago2 degradation. These results suggest that an induced effector protein may need to be continuously generated to maintain low Ago2 protein expression in activated T cells. The ubiquitin ligase Trim71 (a.k.a. mLin41) has been implicated in the regulation of Ago2 stability (Rybak et al., 2009), although two recent studies countered this claim (Chang et al., 2012; Chen et al., 2012). Trim71 mRNA was almost undetectable in resting and restimulated T cells, in comparison to robust expression in embryonic stem (ES) cell–positive control samples (Fig. S3 A). Trim71 protein was also undetectable in T cells, in contrast to ES cell lysate. (Fig. S3 B).

DISCUSSION

Naive T cells that encounter their cognate antigen dramatically remodel their gene expression program as they proliferate and acquire effector functions. The data presented here demonstrate that these cells also actively reset their miRNA repertoire. Activation-induced global posttranscriptional down-regulation of mature miRNAs allows concurrent changes in pri-miRNA gene transcription to rapidly establish a new pattern of miRNA expression in effector cells. Ago1 and Ago2,

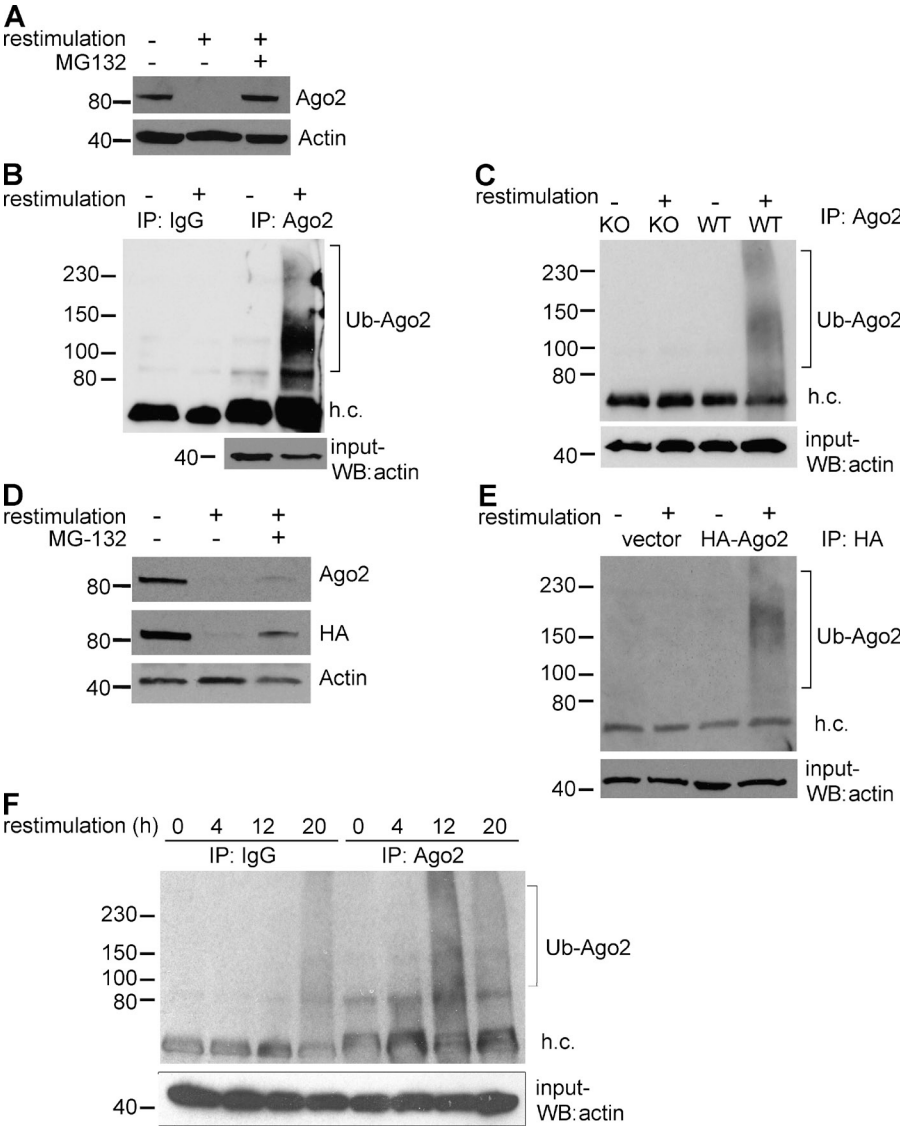

Figure 8. Ago2 is ubiquitinated and degraded by the proteasome. (A) Immunoblot analysis of Ago2 and actin protein in resting, 24 h restimulated T cells, and 24 h restimulated cells with MG-132 added in the last 2 h of culture. (B) IgG (left) or Ago2 (right) immunoprecipitation from resting and 24 h restimulated T cells. All cultures were treated with MG-132 in the last 4 h of culture. Immunoprecipitates were blotted with anti-ubiquitin and 4% input from resting and restimulated cells was blotted with anti-β-actin. Data in A and B are representative of at least five independent experiments. (C) Resting and 24 h restimulated Ago2-deficient (left) or WT (right) T cells. Immunoprecipitation was performed with anti-Ago2 antibody and blotted with anti-ubiquitin antibody. 4% input from resting and restimulated cells was blotted with anti-β-actin. (D) Immunoblot of Ago2, HA, and β-actin from cells transduced with HA-Ago2 retrovirus. Cells were rested until day 5 and restimulated for 24 h with MG-132 or DMSO in the last 4 h of culture. (E) Empty vector (left) and HA-Ago2 retrovirus-transduced (right) T cells that were either rested or restimulated for 24 h. Immunoprecipitation was performed with anti-HA antibody and were blotted with anti-ubiquitin antibody. 4% input from resting and restimulated cells were blotted with anti-β-actin. (F) IgG (left) or Ago2 (right) immunoprecipitation from resting, 4-h, 12-h, and 20-h restimulated T cells. All cultures were treated with MG-132 in the last 4 h of culture. Immunoprecipitates were blotted with anti-ubiquitin, and 4% input from resting and restimulated cells was blotted with anti-β-actin. Data in C–F are representative of two independent experiments. h.c., heavy chain; Ub-Ago2, ubiquitinated Ago2.

which bind miRNAs in the miRISC and mediate target mRNA repression, are also down-regulated during T cell activation in a process of ubiquitination and proteasomal degradation. This degradation depends on intact PI3K/mTOR signaling and continuous transcription and translation. Ago2 is a limiting factor for miRNA expression in T cells, with the abundance of a large panel of miRNAs reduced by 30% for each disrupted allele of *Ago2*. Collectively, our data support a model in which TCR engagement leads to down-regulation of Ago proteins, resulting in decreased miRNA expression. Alternatively, inducible miRNA degradation may destabilize Ago proteins in activated T cells.

These findings have important implications for miRNA regulation of immune responses. Naive $Ago2^{-/-}$ and $Ago2^{+/-}$ T cells appeared to be phenotypically normal at baseline, but were more prone than wild-type cells to differentiate into cytokine-producing effector cells when activated. These data are reminiscent of previous observations of *Dicer*-, *Dgcr8*-, and *Drosha*-deficient cells, which lack essentially all miRNAs and display even more aberrantly unrestrained differentiation, especially into IFN-γ–producing Th1 cells (Muljo et al., 2005; Cobb et al., 2006; Chong et al., 2008; Liston et al., 2008; Zhou et al., 2008; Steiner et al., 2011). Also in accordance with data from *Dicer*-deficient T cells, *Ago2*-deficient T cells have a large percentage of cells producing cytokines that are associated with more than one helper T cell lineage, suggesting a dysfunction in lineage commitment (Muljo et al., 2005). Thus, global miRNA abundance correlates with propensity to differentiate into effector cells, and activation-induced miRISC down-regulation may be important to relax miRNA-mediated gene repression, allowing activated T cells to change their gene expression program and differentiate into effector cells. For example, consider miR-29a, which was among the most highly down-regulated miRNAs in activated T cells. In this context

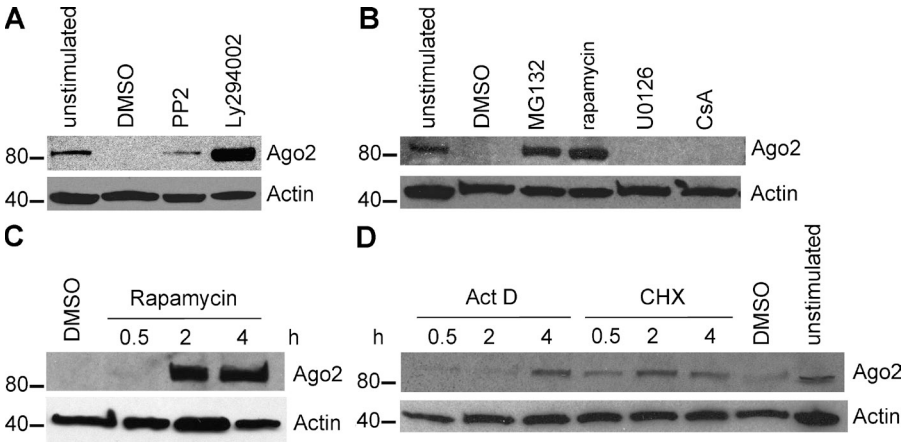

Figure 9. Continuous mTOR signaling is required for Ago2 degradation. (A) Immunoblot analysis of Ago2 and β-actin from resting T cells and T cells restimulated for 16 h plus 4 h treatment with indicated inhibitor. (B) Immunoblot analysis of Ago2 and β-actin from resting T cells and T cells restimulated for 16 h plus 4 h treatment with indicated inhibitor. (C) Immunoblot analysis of Ago2 and β-actin from 16-h restimulated T cells. Cells were then treated with 4 h DMSO (left) or rapamycin for indicated times (right). (D) Immunoblot analysis of Ago2 and β-actin from resting and 16-h restimulated T cells. Cells were then treated with 4-h DMSO (right), actinomycin (left), or cycloheximide (right) for indicated times. Data are representative of at least three independent experiments.

and in Ago2-deficient T cells, decreased miR-29a correlated well with increased expression of its target, T-bet, which is a major determinant of Th1 differentiation and IFN-γ production (Szabo et al., 2003; Steiner et al., 2011). We predict that other miRNAs that are down-regulated during T cell activation play similar roles in restraining Th2 and Th17 gene expression programs. miRNAs may also target common determinants of helper T cell differentiation rather than lineage-specific genes.

In this model, miRNAs expressed in naive T cells act as a "brake" against changes in gene expression, and they are actively eliminated to promote differentiation. However, miRNA-deficient T cells also display survival and proliferation defects, indicating that some miRNAs need to be able to overcome global miRNA down-regulation to support clonal expansion (Muljo et al., 2005; Cobb et al., 2006; Chong et al., 2008; Liston et al., 2008; Zhou et al., 2008; Steiner et al., 2011). Indeed, our data indicate that miRNAs of the miR-17–92 and miR-106a–25 clusters, which can support T cell proliferation and survival in the absence of other miRNAs and are also implicated in lymphoma, are maintained or even up-regulated during T cell activation (He et al., 2005; Xiao et al., 2008; Steiner et al., 2011). Comparison of matched pri-miRNA and mature miRNA measurements indicated that a disproportionately large increase in transcription of these particular miRNA genes offsets the general reduction in miRNA.

miRNAs that cannot compensate with increased transcription during T cell activation are down-regulated relative to their targets (mRNAs) and the translational machinery (rRNA) through a combination of lower Ago protein abundance and dilution with newly transcribed cellular RNAs. To support clonal expansion, activated T cells increase their cellular metabolism, and the total per-cell RNA content increases by ∼10-fold in the first 24–48 h after activation (Frauwirth and Thompson, 2004). Thus, there is major dilution of the existing miRNAs. This effect allows pri-miRNA transcriptional changes to be rapidly translated into changes in mature miRNA levels. This is true not only for up-regulated miRNAs but for those that are transcriptionally repressed. The case of miR-150 illustrates the layered regulation of miRNA expression in activated T cells, and permits an estimation of the rate of miRISC turnover in activated T cells. Primary miR-150 transcription is rapidly silenced in activated T cells, and this combined with Ago down-regulation, dilution with other cellular RNAs, and cell division reduces the abundance of mature miR-150 as a proportion of total RNA to 1–2% of its original level within 2 d. The effect of dilution can be eliminated by considering the amount of miR-150 on a per cell basis, leaving only transcription and mature miRNA elimination as factors in the expression of mature miR-150 over time. Making the conservative assumption that pri-miRNA transcription ceases completely and immediately upon T cell activation, we calculated a half-life between 11 and 18 h for preexisting miR-150 detected by qRT-PCR or Northern blot in several independent experiments (Fig. 1 A, Fig. 2 C, and not depicted). This is considerably shorter than the 12-d half-life of mir-208 in propylthiouracil-treated cardiomyocytes and other estimates that have gained general acceptance in the miRNA research community (van Rooij et al., 2007). The rapid recovery of Ago2 levels upon inhibition of mTOR signaling or proteasome activity suggests that the half-life of miRISC complexes may be as short as 1–2 h at the height of T cell activation.

Our data reveal a crucial and regulated role for Ago proteins in maintaining mature miRNA homeostasis in T cells. Because siRNAs also depend on Ago proteins for their activity, this finding may also have implications for therapeutic siRNA delivery to immune cells. Indeed, shRNA transgenes produce relatively inefficient target gene knockdown in lymphoid organs where T cells and other lymphocytes predominate (Oberdoerffer et al., 2005). Several previous studies used Ago2 deficiency, knockdown, or overexpression to implicate Ago2 as a limiting factor for miRNA expression (Wang et al., 2012). Ago2 is required for normal hematopoiesis, and

Ago2-deficient erythroblasts display a global reduction in miRNAs (O'Carroll et al., 2007). miRNA expression is also reduced in Ago2-deficient mouse embryonic fibroblasts and in Ago-deficient *Xenopus* embryos during early development (Diederichs and Haber, 2007; Lund et al., 2011). Conversely, overexpression of Ago2, but not other proteins in the miRNA biogenesis pathway, increased miRNA expression in HEK293 cells (Diederichs and Haber, 2007). It will be interesting to determine what role Ago2's slicer activity plays in T cells, and whether depletion of other Ago proteins will lead to a similar T cell phenotype.

The ubiquitin ligase Trim71 (mLin41) can ubiquitinate Ago2 in overexpression systems, and siRNA experiments indicated that it may regulate Ago2 abundance and ubiquitination in mouse ES cells (Rybak et al., 2009). However, neither overexpression nor genetic deficiency for Trim71 altered Ago2 expression in neural progenitors (Chen et al., 2012). Moreover, a recent study corroborated these findings in mouse ES cells, and identified a novel function for Trim71 in enhancing miRNA activity (Chang et al., 2012). Our own analyses of Trim71 expression indicate that it is not expressed in T cells. A broader search will be necessary to identify the proteins that mediate Ago2 ubiquitination and degradation in activated T cells.

It is also important to consider whether and how other known posttranslational modifications of Ago proteins may regulate ubiquitination and protein stability in T cells (Qi et al., 2008; Adams et al., 2009; Rybak et al., 2009). Our work has identified an essential role for mTOR signaling in Ago2 down-regulation. This suggests that the mTOR pathway regulates protein synthesis at multiple nodes, both by stimulating ribosome assembly and function, and through inhibiting miRNA activity (Wang and Proud, 2006). Rapamycin, which inhibits mTOR activity, is a potent immunosuppressant that is used to prevent organ rejection (Weichhart and Säemann, 2009). Our work has shown that miRNAs also exhibit immunosuppressive properties, as Ago2-deficient T cells more readily differentiate into cytokine-producing effectors. Thus activation of the miRNA pathway may represent another mode by which rapamycin prevents immune activation. Because the signaling pathways induced by TCR engagement are common to many cell types, it will also be useful to investigate how general this mechanism may be and to determine if other cell types down-regulate Ago proteins and miRNAs upon activation. We note that miRNA turnover is also accelerated in neurons in an activity-dependent manner (Krol et al., 2010). Reduced miRNA abundance is a common feature of many transformed cells, suggesting that Ago protein regulation may also occur in some cancer settings, and contribute to tumorigenesis and metastatic potential (Hwang et al., 2009; Ventura and Jacks, 2009).

MATERIALS AND METHODS

Mice. All mice were housed and bred in specific pathogen–free conditions in the Animal Barrier Facility at the University of California, San Francisco. All animal experiments were approved by the Institutional Animal Care and Use Committee of the University of California, San Francisco. C57BL/6NCr mice were obtained from the National Cancer Institute (Frederick, MD). Ago2 conditional mutant mice (*Eif2c*$^{tm1.1Tara}$) have been described previously (O'Carroll et al., 2007). *CD4-cre* transgenic mice (*Tg(Cd4-cre)1Cwi)* were purchased from Taconic. For in vivo T cell transfer experiments, donors were DO11 TCR transgenics (*Tg(DO11.10)10Dlo*) crossed with Rag2-deficient mice (*Rag2*^{tm1Cgn}; Jackson Laboratories). For recipients, WT BALB/c mice were purchased from Jackson Laboratories. sOVA-transgenic mice (*Tg(Mt1-OVA)#Akab*) were generated as previously described (Villarino et al., 2011)

T cell stimulation and culture. CD4$^+$ T cells from spleen and lymph nodes of young mice (4–7 wk old) were isolated by magnetic bead selection (Invitrogen). Purified CD4$^+$ T cells were stimulated with hamster anti–mouse CD3 (clone 2C11; 0.25 μg/ml) and anti–mouse CD28 (clone 37.51; 1 μg/ml) on plates coated with goat anti–hamster IgG (0.3 mg/ml in PBS for 2 h at room temperature; MP Biomedicals) for 60–68 h at an initial cell density of 0.7–1 × 10^6 cells/ml. After stimulation, cells were expanded in media with 20 U/ml of recombinant IL-2 (National Cancer Institute). ThN (nonpolarizing, no exogenous cytokines or blocking antibodies), low IL-4 (10 U/ml IL-4), low IL-12 (10 pg/ml IL-12), Th1 (10 ng/ml IL-12, 10 μg/ml anti-IL-4) or Th2 (500 U/ml IL-4, 5 μg/ml anti–IFN-γ clone XMG1.2) conditions were maintained throughout stimulation and expansion. The resulting cultures were free of CD8$^+$ T cells (<1%) when analyzed by flow cytometry 5 d after activation. For experiments involving CFSE, cells were labeled for 8 min with 5 μM CFSE, quenched with an equal volume of FBS, and washed two times in 10% FBS before stimulation and culture. For restimulation experiments, cells were stimulated as described above and expanded in IL-2–containing media until 6 d after activation. Cells were harvested and restimulated with anti–mouse CD3 and anti–mouse CD28 on plates coated with goat anti–hamster IgG for the times indicated. For experiments involving inhibitors, cells were restimulated for 16–19.5 h, and inhibitors were added for the last 0.5-4h of restimulation. Inhibitors used were 20 μM PP2, 10 μM LY294002, 100 nM rapamycin, 1 μM Cyclosporin A, 2.5 mg/ml Actinomycin D, 10 μg/ml Cycloheximide, 100 μM U0126, and 10 μM MG-132 (Sigma-Aldrich). All T cell culture was done in DMEM high-glucose media supplemented with 10% FBS, pyruvate, nonessential amino acids, MEM vitamins, L-arginine, L-asparagine, L-glutamine, folic acid, β-mercaptoethanol, penicillin, and streptomycin.

Retroviral transduction. HA-tagged Ago2 cDNA was amplified from RA802B-1_mAGO2_RFP lentiviral plasmid (System Biosciences) and subcloned into pRV-IRES-GFP (plasmid 13249; Addgene). CD4$^+$ cells were stimulated as described for 48 h and transduced with retrovirus produced by Phoenix-E packaging cells transfected with retroviral plasmids. After 5 h of incubation with virus and 5 μg/ml polybrene, media was replaced and cells were cultured and expanded for analysis. A control plasmid was used that lacks HA-tagged Ago2 cDNA.

Transfection and miRNA sensor generation. miRNA sensor constructs were generated by subcloning four perfectly complementary miRNA-binding sites into psiCHECK-2 dual luciferase reporter construct immediately downstream of a renilla luciferase coding gene with each miRNA-binding site separated by 4 bp. CD4$^+$ T cells were stimulated in vitro for the indicated times and transfected with miRNA sensor constructs. Cells were transfected using the Neon electroporation transfection system (Invitrogen) with an optimized version of the manufacturers recommended protocol. In brief, transfections were performed using 4 × 10^7 cells in 10 μl "R buffer" (Invitrogen) with 333 ng of plasmid DNA. Optimized Neon transfection system setting was 1,550 V with three 10-ms pulses. For transfection, cells were removed from plates, transfected, and returned to fresh plate-bound stimulation (anti-CD3, anti-CD28). Luciferase activity was measured 18 h after transfection using the Dual Luciferase Reporter Assay System (Promega) and a FLUOstar Optima plate reader (BMG Labtech).

Adoptive transfers and immunizations. LNs and spleens were pooled from 4–6-wk-old DO11 *Rag2*$^{-/-}$ mice and CD4$^+$ cells purified (>96% purity) by positive selection using magnetic beads (Invitrogen). 2–5 × 10^5 CD4$^+$

cells were then intravenously injected into age- and sex-matched recipients (in 400 µl PBS). For immunizations, donor T cells were transferred into WT BALB/c mice and, 24 h later, they were immunized (i.v.) with 1–5 × 10^5 BM-derived DCs that were preactivated with LPS and loaded with OVA peptide (1 g/ml each; Sigma-Aldrich).

Ex vivo T cell monitoring. $CD4^+$ cells were enriched from pooled LNs and spleens of recipient mice (days 4–5 posttransfer) and stained directly ex vivo with fluorochrome-labeled anti-CD4, anti-CD44, and anti-DO11.10 antibodies (eBioscience). High-speed cell sorting was then used to purify $CD4^+$ $DO11.10^+$ $CD44^{hi}$ cells (<95% purity). For all experiments, naive controls were obtained from LNs and/or spleen of DO11.10 mice (no adoptive transfer) and defined as $CD4^+$ $DO11.10^+$ $CD44^{lo}$ (>99% purity). For ELISAs, purified T cells were stimulated overnight with LPS/OVA-pulsed, BM-derived DCs (5:1 T cell/DC ratio), and cytokine concentrations were measured in supernatants using standard methodologies (antibody pairs from eBioscience).

miRNA arrays. For in vitro analyses, total RNA was extracted from naive and in vitro–activated mouse and human T cells. For ex vivo analyses, 0.5 × 10^6 donor T cells ($CD4^+$ $D011.10^+$ $CD44^{hi}$ cells from sOVA and immunized hosts) and 1 × 10^6 naive T controls ($CD4^+$ $D011.10^+$ $CD25^-$ $CD44^{lo}$ cells from DO11.10 *Rag2*$^{+/+}$mice) were purified by high-speed cell sorting. Quality control was performed using an Agilent 2100 Bioanalyzer (Agilent Technologies), and RNA was labeled with Cy3-CTP using the miRCURY LNA miRNA power labeling kit (Exiqon, Inc.), according to the manufacturer's protocol. Labeled RNA (250 ng/well) was then hybridized to Agilent custom UCSF miRNA v3.3 multi-species 8 × 15K ink-jet arrays. Hybridizations were performed for 16 h, according to the manufacturer's protocol. Arrays were scanned using the Agilent microarray scanner and raw signal intensities were extracted with Feature Extraction software.

Data analysis. For in vitro microarray analyses, no background subtraction was performed, and the median feature pixel intensity was used as the raw signal before quantile normalization. A filter was used to remove probes with a max log2 signal across arrays of <6. This filter prevents the prevalence of so many low-intensity probes, which tend to have smaller variance, from underestimating global and per-gene estimates of variance. Each array's signal was normalized to the median interpolated tRNA signal. First, the miRNA probes were quantile normalized without the tRNA probes. Next, a linear interpolation function between the raw miRNA signal and the normalized data were created. This function was evaluated with the raw tRNA signal values to produce the interpolated tRNA probe values. Within each array, the median tRNA value across tRNA probes was used as the basis of comparison for all miRNA probes on that array.

For ex vivo analyses, tRNA probes were not present, and data were normalized using the quantile normalization method with a filter to remove all probes where the max log2 signal across arrays was <6 (Bolstad et al., 2003). Microarray data were submitted to the Gene Expression Omnibus database (accession nos. GSE36606 and GSE36607).

RNA isolation and qRT-PCR. For in vitro–activated T cells, total RNA was isolated with TRIzol LS reagent (Invitrogen) from naive and stimulated T cells. Sequences of all primers used for PCR are provided in Table S1. For mRNA expression, total RNA was oligo(dT)-primed for first strand cDNA synthesis (Superscript III kit; Invitrogen). For mature miRNA expression analysis, total RNA was subjected to polyA addition and cDNA synthesis (NCode kit; Invitrogen). qRT-PCR was performed using one miRNA-specific primer and one constant primer (corresponding to the modified oligo-dT) with SYBR Green master mix (Roche) and a Realplex2 thermocycler (Eppendorf). For pre-miRNA and pri-miRNA expression analysis, total RNA was fractionated into a large and small fraction (miRNeasy kit; QIAGEN) and random hexamer-primed for first-strand cDNA synthesis. pri-miRNA qRT-PCR was performed using primers spanning one arm of the stem loop, and the flanking sequence on cDNA synthesized from the large RNA fraction. Pre-miRNA qRT-PCR was performed using primers within the stem loop on cDNA synthesized from the small RNA fraction. Dilution series were performed to confirm linear performance of these qRT-PCR assays. Pri-miRNAs were below the limit of detection in all small RNA fraction samples. For in vivo–activated T cells, PCR amplification was performed with SYBR Green master mix (5–10 ng cDNA per reaction; Applied Biosystems) using an iQ5 Real-Time PCR thermal cycler (Bio-Rad Laboratories). Reactions were performed in duplicate, and threshold cycle (Ct) values normalized to 5.8S or 18S rRNA for mature miRNAs, 5S for pre-miRNAs, 28S for pri-miRNAs, and β-actin for mRNAs. Trim71 qRT-PCR was performed using TaqMan Gene Expression Assay Mm01341471_m1 (Applied Biosystems).

Intracellular staining and antibodies. For intracellular cytokine analysis, cells were restimulated for 4 h with 10 nM PMA and 1 µM ionomycin in the presence of 5 µg/ml brefeldin A to allow intracellular cytokine accumulation. For all cytokine stains, cells were fixed with 4% formaldehyde and subsequently permeabilized and stained in PBS containing 0.5% saponin, 1% bovine serum albumin, and 0.1% sodium azide. For intracellular T-bet stains, cells were fixed and stained with the Foxp3 Staining Buffer Set (eBioscience). Fluorophore-conjugated antibodies including eFluro450-IFN-γ, allophycocyanin (APC)-IL-4, PE-IL-13, and APC-T-bet were obtained from eBioscience. Stained cells were analyzed with a LSRII and FACSDiva software (BD) as well as FlowJo analysis software (Tree Star).

Cell extracts and immunoblot analysis. Cells were lysed in 0.5% Nonidet P40, 150 mM NaCl, 50 mM Tris, pH 8.0, 5 mM EDTA, 1 mM phenylmethylsulfonyl fluoride, 25 µg/ml of aprotinin, 25 µg/ml of leupeptin, 10 mM NaF, 8 mM β-glycerophosphate for 15 min. Lysates were cleared by centrifugation, resolved on 4–15% gradient SDS-PAGE gels, and transferred onto nitrocellulose membranes (Schleicher and Schuell). Membranes were blocked with 5% powdered milk in TBS (10 mM Tris-HCl, pH 8.0, and 150 mM NaCl), incubated with antibodies diluted in blocking solution, and washed with TBS containing 0.1% Tween-20. Antibodies used were anti–β-actin (A5441; Sigma-Aldrich), HRP donkey anti–mouse IgG (Jackson Laboratories), HRP Donkey anti-mouse IgM (Jackson ImmunoResearch), HRP goat anti-rabbit IgG (Jackson ImmunoResearch), anti-TRBP (72110; Abcam), HRP goat anti–rat IgG (Jackson ImmunoResearch), anti-Drosha (12286; Abcam), anti-Ago2 (Cell Signaling Technology), anti-Ago1 (4B8, gift of G. Meister, Max-Planck-Institute of Biochemistry, Martinsreid, Germany), rat anti–mouse pan-Ago (11G1) for immunoblot analysis. Anti-Ago2 (Wako Chemicals USA), anti-Trim71 (R&D Systems), anti-HA (clone 3F10; Roche), and mouse IgG (Abcam) were used for immunoprecipitations.

Ubiquitination assays and immunoprecipitations. For endogenous Ago2 ubiquitination assays, cells were taken off stimulation at 72 h and expanded in culture until day 6. Cells were returned to fresh plate-bound stimulation (anti-CD3, anti-CD28) for 16 h, at which point 10 µM MG-132 or DMSO control was added for 4 h. Alternatively, cells were returned to fresh IL-2–containing media for 16 h and MG-132 was added for 4 h more. For overexpressed HA-Ago2 ubiquitination assays, cells were taken off stimulation at day 2 after 5-h incubation with retrovirus, expanded in culture until day 5, and restimulated as described above. Cells were lysed in pre-boiled lysis buffer (25 mM Hepes, pH 7.5, 150 mM NaCl, 0.5 mM EDTA, 1% SDS, 0.1% NP-40, 1 mM phenylmethylsulfonyl fluoride, 25 µg/ml of aprotinin, 25 µg/ml of leupeptin, 10 mM NaF, 8 mM β-glycerophosphate, 1 mM sodium vanadate, 1 mM dithiothreitol, 10 µM MG-132, and 5 mM NEM for 15 min) and incubated for 5 min at 95°C to disrupt noncovalent interactions. Lysates were diluted 1:10 with NP-40 buffer (25 mM Hepes, pH 7.5, 150 mM NaCl, 0.2% NP-40, 10% glycerol, 1 mM phenylmethylsulfonyl fluoride, 25 µg/ml aprotinin, 25 µg/ml leupeptin, 10 mM NaF, 8 mM β-glycerophosphate, 1 mM sodium vanadate, 1 mM dithiothreitol, 10 µM MG-132, and 5 mM NEM), passed through a needle and syringe to fragment DNA, clarified by centrifugation at 18,800 *g* for 10 min, and incubated overnight with antibody (10 µg anti-Ago21 or 1 µg anti-HA at 4°C. Immunoprecipitates were collected with protein G magnetic beads (Dynabeads; Invitrogen) for 1 h at 4°C, washed, and analyzed by Western blotting.

Mouse ES cells. Mouse ES cell protein and cDNA samples were provided by R. Krishnakumar (University of California at San Francisco, San Francisco, CA). ES cells were V6.5 mouse ES cells grown in 15% FBS and supplemented with Lif and 2i. cDNA was prepared using random hexamer primers.

Online supplemental material. Fig. S1 demonstrates the specificity of the newly generated anti–mouse pan-Ago monoclonal antibody. Fig. S2 shows the gating strategy for isolating OVA-specific naive and effector T cells, and phenotypic characterization of the effector cells. Fig. S3 shows the expression of Trim71 in T cells. Primer sequences used in qRT-PCR analyses are provided in Table S1. Online supplemental material is available at http://www.jem.org/cgi/content/full/jem.20111717/DC1.

The authors thank Marisella Panduro-Sicheva, Sarah Abdul-Wajid, and Laura Smith for technical assistance; Mehrdad Matloubian for critical reading of the manuscript; and Michael McManus and members of the University of California at San Francisco miRNA in lymphocytes interest group for helpful discussions.

This work was supported by the National Institutes of Health (R56AI089828 and R01HL109102 to K.M. Ansel; R01DA026065 and R01GM08078 to M.T. McManus), the Dana Foundation (K.M. Ansel), the Burroughs Wellcome Fund (CABS 1006173 to K.M. Ansel), the University of California San Francisco Program for Breakthrough Biomedical Research (K.M. Ansel, D.J. E.rele, and A.V. Villarino), the Sandler Asthma Basic Research Center, and the German Research Foundation (DFG HE 3359/3-1 to V. Heissmeyer). Y. Bronevetsky is a National Science Foundation predoctoral fellow (2009057510). G. Heinz is supported by the Boehringer Ingelheim Foundation.

The authors have no conflicting financial interests.

Submitted: 10 April 2012
Accepted: 17 December 2012

REFERENCES

Adams, B.D., K.P. Claffey, and B.A. White. 2009. Argonaute-2 expression is regulated by epidermal growth factor receptor and mitogen-activated protein kinase signaling and correlates with a transformed phenotype in breast cancer cells. *Endocrinology*. 150:14–23. http://dx.doi.org/10.1210/en.2008-0984

Ansel, K.M., I. Djuretic, B. Tanasa, and A. Rao. 2006. Regulation of Th2 differentiation and Il4 locus accessibility. *Annu. Rev. Immunol.* 24:607–656. http://dx.doi.org/10.1146/annurev.immunol.23.021704.115821

Banerjee, A., F. Schambach, C.S. DeJong, S.M. Hammond, and S.L. Reiner. 2010. Micro-RNA-155 inhibits IFN-gamma signaling in CD4+ T cells. *Eur. J. Immunol.* 40:225–231. http://dx.doi.org/10.1002/eji.200939381

Barski, A., R. Jothi, S. Cuddapah, K. Cui, T.Y. Roh, D.E. Schones, and K. Zhao. 2009. Chromatin poises miRNA- and protein-coding genes for expression. *Genome Res.* 19:1742–1751. http://dx.doi.org/10.1101/gr.090951.109

Bartel, D.P. 2009. MicroRNAs: target recognition and regulatory functions. *Cell.* 136:215–233. http://dx.doi.org/10.1016/j.cell.2009.01.002

Bas, A., G. Forsberg, S. Hammarström, and M.L. Hammarström. 2004. Utility of the housekeeping genes 18S rRNA, beta-actin and glyceraldehyde-3-phosphate-dehydrogenase for normalization in real-time quantitative reverse transcriptase-polymerase chain reaction analysis of gene expression in human T lymphocytes. *Scand. J. Immunol.* 59:566–573. http://dx.doi.org/10.1111/j.0300-9475.2004.01440.x

Bolstad, B.M., R.A. Irizarry, M. Astrand, and T.P. Speed. 2003. A comparison of normalization methods for high density oligonucleotide array data based on variance and bias. *Bioinformatics*. 19:185–193. http://dx.doi.org/10.1093/bioinformatics/19.2.185

Brunn, G.J., J. Williams, C. Sabers, G. Wiederrecht, J.C. Lawrence Jr., and R.T. Abraham. 1996. Direct inhibition of the signaling functions of the mammalian target of rapamycin by the phosphoinositide 3-kinase inhibitors, wortmannin and LY294002. *EMBO J.* 15:5256–5267.

Chang, T.C., D. Yu, Y.S. Lee, E.A. Wentzel, D.E. Arking, K.M. West, C.V. Dang, A. Thomas-Tikhonenko, and J.T. Mendell. 2008. Widespread microRNA repression by Myc contributes to tumorigenesis. *Nat. Genet.* 40:43–50. http://dx.doi.org/10.1038/ng.2007.30

Chang, H.M., N.J. Martinez, J.E. Thornton, J.P. Hagan, K.D. Nguyen, and R.I. Gregory. 2012. Trim71 cooperates with microRNAs to repress Cdkn1a expression and promote embryonic stem cell proliferation. *Nat. Commun.* 3:923. http://dx.doi.org/10.1038/ncomms1909

Chen, J., F. Lai, and L. Niswander. 2012. The ubiquitin ligase mLin41 temporally promotes neural progenitor cell maintenance through FGF signaling. *Genes Dev.* 26:803–815. http://dx.doi.org/10.1101/gad.187641.112

Chong, M.M., J.P. Rasmussen, A.Y. Rudensky, and D.R. Littman. 2008. The RNAseIII enzyme Drosha is critical in T cells for preventing lethal inflammatory disease. *J. Exp. Med.* 205:2005–2017. http://dx.doi.org/10.1084/jem.20081219

Cobb, B.S., A. Hertweck, J. Smith, E. O'Connor, D. Graf, T. Cook, S.T. Smale, S. Sakaguchi, F.J. Livesey, A.G. Fisher, and M. Merkenschlager. 2006. A role for Dicer in immune regulation. *J. Exp. Med.* 203:2519–2527. http://dx.doi.org/10.1084/jem.20061692

Davis, B.N., A.C. Hilyard, G. Lagna, and A. Hata. 2008. SMAD proteins control DROSHA-mediated microRNA maturation. *Nature.* 454:56–61. http://dx.doi.org/10.1038/nature07086

Diederichs, S., and D.A. Haber. 2007. Dual role for argonautes in microRNA processing and posttranscriptional regulation of microRNA expression. *Cell.* 131:1097–1108. http://dx.doi.org/10.1016/j.cell.2007.10.032

Frauwirth, K.A., and C.B. Thompson. 2004. Regulation of T lymphocyte metabolism. *J. Immunol.* 172:4661–4665.

Ghodgaonkar, M.M., R.G. Shah, F. Kandan-Kulangara, E.B. Affar, H.H. Qi, E. Wiemer, and G.M. Shah. 2009. Abrogation of DNA vector-based RNAi during apoptosis in mammalian cells due to caspase-mediated cleavage and inactivation of Dicer-1. *Cell Death Differ.* 16:858–868. http://dx.doi.org/10.1038/cdd.2009.15

Haasch, D., Y.W. Chen, R.M. Reilly, X.G. Chiou, S. Koterski, M.L. Smith, P. Kroeger, K. McWeeny, D.N. Halbert, K.W. Mollison, et al. 2002. T cell activation induces a noncoding RNA transcript sensitive to inhibition by immunosuppressant drugs and encoded by the proto-oncogene, BIC. *Cell. Immunol.* 217:78–86. http://dx.doi.org/10.1016/S0008-8749(02)00506-3

Han, J., J.S. Pedersen, S.C. Kwon, C.D. Belair, Y.K. Kim, K.H. Yeom, W.Y. Yang, D. Haussler, R. Blelloch, and V.N. Kim. 2009. Posttranscriptional crossregulation between Drosha and DGCR8. *Cell.* 136:75–84. http://dx.doi.org/10.1016/j.cell.2008.10.053

He, L., J.M. Thomson, M.T. Hemann, E. Hernando-Monge, D. Mu, S. Goodson, S. Powers, C. Cordon-Cardo, S.W. Lowe, G.J. Hannon, and S.M. Hammond. 2005. A microRNA polycistron as a potential human oncogene. *Nature.* 435:828–833. http://dx.doi.org/10.1038/nature03552

Hoefig, K.P., and V. Heissmeyer. 2008. MicroRNAs grow up in the immune system. *Curr. Opin. Immunol.* 20:281–287. http://dx.doi.org/10.1016/j.coi.2008.05.005

Hwang, H.W., E.A. Wentzel, and J.T. Mendell. 2009. Cell-cell contact globally activates microRNA biogenesis. *Proc. Natl. Acad. Sci. USA.* 106:7016–7021. http://dx.doi.org/10.1073/pnas.0811523106

Kim, V.N., J. Han, and M.C. Siomi. 2009. Biogenesis of small RNAs in animals. *Nat. Rev. Mol. Cell Biol.* 10:126–139. http://dx.doi.org/10.1038/nrm2632

Krol, J., V. Busskamp, I. Markiewicz, M.B. Stadler, S. Ribi, J. Richter, J. Duebel, S. Bicker, H.J. Fehling, D. Schübeler, et al. 2010. Characterizing light-regulated retinal microRNAs reveals rapid turnover as a common property of neuronal microRNAs. *Cell.* 141:618–631. http://dx.doi.org/10.1016/j.cell.2010.03.039

Kuchen, S., W. Resch, A. Yamane, N. Kuo, Z. Li, T. Chakraborty, L. Wei, A. Laurence, T. Yasuda, S. Peng, et al. 2010. Regulation of microRNA expression and abundance during lymphopoiesis. *Immunity.* 32:828–839. http://dx.doi.org/10.1016/j.immuni.2010.05.009

Liston, A., L.F. Lu, D. O'Carroll, A. Tarakhovsky, and A.Y. Rudensky. 2008. Dicer-dependent microRNA pathway safeguards regulatory T cell function. *J. Exp. Med.* 205:1993–2004. http://dx.doi.org/10.1084/jem.20081062

Lu, L.F., M.P. Boldin, A. Chaudhry, L.L. Lin, K.D. Taganov, T. Hanada, A. Yoshimura, D. Baltimore, and A.Y. Rudensky. 2010. Function of miR-146a in controlling Treg cell-mediated regulation of Th1 responses. *Cell.* 142:914–929. http://dx.doi.org/10.1016/j.cell.2010.08.012

Lund, E., M.D. Sheets, S.B. Imboden, and J.E. Dahlberg. 2011. Limiting Ago protein restricts RNAi and microRNA biogenesis during early

development in Xenopus laevis. *Genes Dev.* 25:1121–1131. http://dx.doi.org/10.1101/gad.2038811

Monticelli, S., K.M. Ansel, C. Xiao, N.D. Socci, A.M. Krichevsky, T.H. Thai, N. Rajewsky, D.S. Marks, C. Sander, K. Rajewsky, et al. 2005. MicroRNA profiling of the murine hematopoietic system. *Genome Biol.* 6:R71. http://dx.doi.org/10.1186/gb-2005-6-8-r71

Muljo, S.A., K.M. Ansel, C. Kanellopoulou, D.M. Livingston, A. Rao, and K. Rajewsky. 2005. Aberrant T cell differentiation in the absence of Dicer. *J. Exp. Med.* 202:261–269. http://dx.doi.org/10.1084/jem.20050678

O'Carroll, D., I. Mecklenbrauker, P.P. Das, A. Santana, U. Koenig, A.J. Enright, E.A. Miska, and A. Tarakhovsky. 2007. A Slicer-independent role for Argonaute 2 in hematopoiesis and the microRNA pathway. *Genes Dev.* 21:1999–2004. http://dx.doi.org/10.1101/gad.1565607

O'Connell, R.M., D.S. Rao, A.A. Chaudhuri, and D. Baltimore. 2010. Physiological and pathological roles for microRNAs in the immune system. *Nat. Rev. Immunol.* 10:111–122. http://dx.doi.org/10.1038/nri2708

Oberdoerffer, P., C. Kanellopoulou, V. Heissmeyer, C. Paeper, C. Borowski, I. Aifantis, A. Rao, and K. Rajewsky. 2005. Efficiency of RNA interference in the mouse hematopoietic system varies between cell types and developmental stages. *Mol. Cell. Biol.* 25:3896–3905. http://dx.doi.org/10.1128/MCB.25.10.3896-3905.2005

Paroo, Z., X. Ye, S. Chen, and Q. Liu. 2009. Phosphorylation of the human microRNA-generating complex mediates MAPK/Erk signaling. *Cell.* 139:112–122. http://dx.doi.org/10.1016/j.cell.2009.06.044

Qi, H.H., P.P. Ongusaha, J. Myllyharju, D. Cheng, O. Pakkanen, Y. Shi, S.W. Lee, J. Peng, and Y. Shi. 2008. Prolyl 4-hydroxylation regulates Argonaute 2 stability. *Nature.* 455:421–424. http://dx.doi.org/10.1038/nature07186

Rodriguez, A., E. Vigorito, S. Clare, M.V. Warren, P. Couttet, D.R. Soond, S. van Dongen, R.J. Grocock, P.P. Das, E.A. Miska, et al. 2007. Requirement of bic/microRNA-155 for normal immune function. *Science.* 316:608–611. http://dx.doi.org/10.1126/science.1139253

Rossi, R.L., G. Rossetti, L. Wenandy, S. Curti, A. Ripamonti, R.J. Bonnal, R.S. Birolo, M. Moro, M.C. Crosti, P. Gruarin, et al. 2011. Distinct microRNA signatures in human lymphocyte subsets and enforcement of the naive state in CD4+ T cells by the microRNA miR-125b. *Nat. Immunol.* 12:796–803. http://dx.doi.org/10.1038/ni.2057

Rüdel, S., Y. Wang, R. Lenobel, R. Körner, H.H. Hsiao, H. Urlaub, D. Patel, and G. Meister. 2011. Phosphorylation of human Argonaute proteins affects small RNA binding. *Nucleic Acids Res.* 39:2330–2343. http://dx.doi.org/10.1093/nar/gkq1032

Rybak, A., H. Fuchs, K. Hadian, L. Smirnova, E.A. Wulczyn, G. Michel, R. Nitsch, D. Krappmann, and F.G. Wulczyn. 2009. The let-7 target gene mouse lin-41 is a stem cell specific E3 ubiquitin ligase for the miRNA pathway protein Ago2. *Nat. Cell Biol.* 11:1411–1420. http://dx.doi.org/10.1038/ncb1987

Shi, L., L.H. Reid, W.D. Jones, R. Shippy, J.A. Warrington, S.C. Baker, P.J. Collins, F. de Longueville, E.S. Kawasaki, K.Y. Lee, et al; MAQC Consortium. 2006. The MicroArray Quality Control (MAQC) project shows inter- and intraplatform reproducibility of gene expression measurements. *Nat. Biotechnol.* 24:1151–1161. http://dx.doi.org/10.1038/nbt1239

Steiner, D.F., M.F. Thomas, J.K. Hu, Z. Yang, J.E. Babiarz, C.D. Allen, M. Matloubian, R. Blelloch, and K.M. Ansel. 2011. MicroRNA-29 regulates T-box transcription factors and interferon-γ production in helper T cells. *Immunity.* 35:169–181. http://dx.doi.org/10.1016/j.immuni.2011.07.009

Stetson, D.B., D. Voehringer, J.L. Grogan, M. Xu, R.L. Reinhardt, S. Scheu, B.L. Kelly, and R.M. Locksley. 2004. Th2 cells: orchestrating barrier immunity. *Adv. Immunol.* 83:163–189. http://dx.doi.org/10.1016/S0065-2776(04)83005-0

Stittrich, A.B., C. Haftmann, E. Sgouroudis, A.A. Kühl, A.N. Hegazy, I. Panse, R. Riedel, M. Flossdorf, J. Dong, F. Fuhrmann, et al. 2010. The microRNA miR-182 is induced by IL-2 and promotes clonal expansion of activated helper T lymphocytes. *Nat. Immunol.* 11:1057–1062. http://dx.doi.org/10.1038/ni.1945

Szabo, S.J., B.M. Sullivan, S.L. Peng, and L.H. Glimcher. 2003. Molecular mechanisms regulating Th1 immune responses. *Annu. Rev. Immunol.* 21:713–758. http://dx.doi.org/10.1146/annurev.immunol.21.120601.140942

Taganov, K.D., M.P. Boldin, K.J. Chang, and D. Baltimore. 2006. NF-kappaB-dependent induction of microRNA miR-146, an inhibitor targeted to signaling proteins of innate immune responses. *Proc. Natl. Acad. Sci. USA.* 103:12481–12486. http://dx.doi.org/10.1073/pnas.0605298103

Thai, T.H., D.P. Calado, S. Casola, K.M. Ansel, C. Xiao, Y. Xue, A. Murphy, D. Frendewey, D. Valenzuela, J.L. Kutok, et al. 2007. Regulation of the germinal center response by microRNA-155. *Science.* 316:604–608. http://dx.doi.org/10.1126/science.1141229

Thomson, J.M., M. Newman, J.S. Parker, E.M. Morin-Kensicki, T. Wright, and S.M. Hammond. 2006. Extensive post-transcriptional regulation of microRNAs and its implications for cancer. *Genes Dev.* 20:2202–2207. http://dx.doi.org/10.1101/gad.1444406

Trabucchi, M., P. Briata, M. Garcia-Mayoral, A.D. Haase, W. Filipowicz, A. Ramos, R. Gherzi, and M.G. Rosenfeld. 2009. The RNA-binding protein KSRP promotes the biogenesis of a subset of microRNAs. *Nature.* 459:1010–1014. http://dx.doi.org/10.1038/nature08025

van Rooij, E., L.B. Sutherland, X. Qi, J.A. Richardson, J. Hill, and E.N. Olson. 2007. Control of stress-dependent cardiac growth and gene expression by a microRNA. *Science.* 316:575–579. http://dx.doi.org/10.1126/science.1139089

Ventura, A., and T. Jacks. 2009. MicroRNAs and cancer: short RNAs go a long way. *Cell.* 136:586–591. http://dx.doi.org/10.1016/j.cell.2009.02.005

Villarino, A.V., S.D. Katzman, E. Gallo, O. Miller, S. Jiang, M.T. McManus, and A.K. Abbas. 2011. Posttranscriptional silencing of effector cytokine mRNA underlies the anergic phenotype of self-reactive T cells. *Immunity.* 34:50–60. http://dx.doi.org/10.1016/j.immuni.2010.12.014

Wang, X., and C.G. Proud. 2006. The mTOR pathway in the control of protein synthesis. *Physiology (Bethesda).* 21:362–369. http://dx.doi.org/10.1152/physiol.00024.2006

Wang, D., Z. Zhang, E. O'Loughlin, T. Lee, S. Houel, D. O'Carroll, A. Tarakhovsky, N.G. Ahn, and R. Yi. 2012. Quantitative functions of Argonaute proteins in mammalian development. *Genes Dev.* 26:693–704. http://dx.doi.org/10.1101/gad.182758.111

Weichhart, T., and M.D. Säemann. 2009. The multiple facets of mTOR in immunity. *Trends Immunol.* 30:218–226. http://dx.doi.org/10.1016/j.it.2009.02.002

Wilson, C.B., E. Rowell, and M. Sekimata. 2009. Epigenetic control of T-helper-cell differentiation. *Nat. Rev. Immunol.* 9:91–105. http://dx.doi.org/10.1038/nri2487

Xiao, C., L. Srinivasan, D.P. Calado, H.C. Patterson, B. Zhang, J. Wang, J.M. Henderson, J.L. Kutok, and K. Rajewsky. 2008. Lymphoproliferative disease and autoimmunity in mice with increased miR-17-92 expression in lymphocytes. *Nat. Immunol.* 9:405–414. http://dx.doi.org/10.1038/ni1575

Zhou, X., L.T. Jeker, B.T. Fife, S. Zhu, M.S. Anderson, M.T. McManus, and J.A. Bluestone. 2008. Selective miRNA disruption in T reg cells leads to uncontrolled autoimmunity. *J. Exp. Med.* 205:1983–1991. http://dx.doi.org/10.1084/jem.20080707

Zhu, J., and W.E. Paul. 2010. Peripheral CD4+ T-cell differentiation regulated by networks of cytokines and transcription factors. *Immunol. Rev.* 238:247–262. http://dx.doi.org/10.1111/j.1600-065X.2010.00951.x